Zootaxa 4590 (5): 501–524
https://www.mapress.com/j/zt/

Article

ISSN 1175-5326 (print edition)
ZOOTAXA
ISSN 1175-5334 (online edition)

https://doi.org/10.11646/zootaxa.4590.5.1
http://zoobank.org/urn:lsid:zoobank.org:pub:F484C560-CAE9-4A9E-B408-AEC2C8893DAD

Redescription and taxonomic status of *Dipturus chilensis* (Guichenot, 1848), and description of *Dipturus lamillai* sp. nov. (Rajiformes: Rajidae), a new species of long-snout skate from the Falkland Islands

FRANCISCO J. CONCHA[1,2,7], JANINE N. CAIRA[1], DAVID A. EBERT[3,4,5] & JOOST H. W. POMPERT[6]

[1]*Department of Ecology & Evolutionary Biology, University of Connecticut, 75 North Eagleville Road, Unit 3043 Storrs, CT 06269 – 3043, USA*
[2]*Facultad de Ciencias del Mar y de Recursos Naturales, Universidad de Valparaíso, Av. Borgoño 16344, Viña del Mar, Chile*
[3]*Pacific Shark Research Center, Moss Landing Marine Laboratories, Moss Landing, CA 95039, USA*
[4]*Department of Ichthyology, California Academy of Sciences, 55 Music Concourse Drive, San Francisco, CA 94118, USA*
[5]*South African Institute for Aquatic Biodiversity, Private Bag 1015, Grahamstown 6140, South Africa*
[6]*Georgia Seafoods Ltd, Waverley House, Stanley, Falkland Islands, United Kingdom*
[7]*Corresponding author. E-mail: francisco.concha@uv.cl*

Abstract

Recent molecular evidence has called into question the identity of skates collected in the waters off the Falkland Islands previously identified as *Zearaja chilensis*. NADH2 sequence data indicate that these specimens are not conspecific with those currently referred to as *Z. chilensis* from Chile and, in fact, represent a novel cryptic species. This study aimed to investigate this hypothesis based on morphological comparisons of specimens from the coasts of both western and eastern South America. In total, 50 specimens from Chile and 41 specimens from the Falkland Islands were collected and examined; morphometric data were generated for a subset of specimens from both areas. NADH2 sequence data were generated for a total of 19 specimens from both areas, as well as specimens of *Z. nasuta* from New Zealand, *D. pullopunctatus* from South Africa, *D. oxyrinchus* from the Azores, *Okamejei hollandi*, and *O. cairae* from Borneo, and *O. kenojei* from Japan. Based on morphological and molecular analyses, *Zearaja* is synonymized with *Dipturus* and species assigned to the former genus are transferred to the latter genus. A neotype is designated for *D. chilensis* and this species is redescribed. *Dipturus lamillai* **sp. nov.** is described based on specimens from the Falkland Islands. Comparison of our NADH2 data with data for mitochondrial genomes generated from tissue samples taken from two specimens originally identified as *Z. chilensis*, indicate that, while the sample from Chile came from a specimen of *D. chilensis,* that from the skate steak obtained from a restaurant in Korea actually came from a specimen of *D. lamillai* **sp. nov.** This emphasizes the importance of confirming both the provenance and identity of specimens from which sequence data are generated and submitted to GenBank if misidentifications are to be avoided.

Key words: Chondrichthyes, batoids, long-nosed skates, southeastern Pacific, diversification patterns, taxonomy

Introduction

Long-nosed skates of the genus *Dipturus* Rafinesque 1810 are relatively large skates distributed worldwide from temperate to tropical waters, mostly on continental shelves and slopes (Last & Yearsley 2002; Ebert & Compagno 2007). Recent taxonomic accounts for batoids indicate that the genus *Dipturus*, with 38 valid species, is surpassed in diversity among Rajiformes only by *Bathyraja* Ishiyama 1958, with 54 valid species (Last *et al.* 2016). To date, nine species of *Dipturus* have been reported in the waters off South America: *D. argentinensis* Díaz de Astarloa, Mabragaña, Hanner & Figueroa 2008, *D. bullisi* (Bigelow & Schroeder 1962), *D. chilensis* (Guichenot 1848), *D. ecuadoriensis* (Beebe & Tee-Van 1941), *D. garricki* (Bigelow & Schroeder 1958), *D. leptocaudus* (Krefft & Stehmann 1975), *D. mennii* (Gomes & Paragó 2001), *D. teevani* (Bigelow & Schroeder 1951), and *D. trachydermus* (Krefft & Stehmann 1975). However, recent barcoding (Naylor *et al.* 2012a) and molecular phylogenetic works (Naylor *et al.* 2012b) suggest the presence of a cryptic species in the southwestern Atlantic

Accepted by M.R. de Carvalho: 7 Feb. 2019; published: 1 May 2019

Ocean. The taxon in question is the yellow-nose skate, *D. chilensis*, whose taxonomic history was extensively reviewed by Vargas-Caro *et al.* (2015). Historically, this species has been considered to occur on the continental shelf from central Chile to southern Brazil (Gomes & Picado 2001; Licandeo & Cerna 2007; Cousseau *et al.* 2007) including the Falkland Islands (Menni *et al.* 2010; Pompert *et al.* 2014).

Recent analyses of sequence data from the protein-coding gene nicotidamide adenine dinucleotide dehydrogenase subunit 2 (NADH2) have provided new insights into the taxonomy and phylogenetic relationships of cartilaginous fishes and, relevant here, skates of the genus *Dipturus*. Naylor *et al.* (2012a) found an average pairwise p-distance of 29.5 base pairs between eight specimens of *D. chilensis* from Chile (which they referred to as *Zearaja chilensis*) and three specimens from the Falkland Islands (which they referred to as *Zearaja flavirostris* [Philippi 1892]). Furthermore, in their phylogenetic analysis of NADH2 data, Naylor *et al.* (2012b) found their exemplar of *D. chilensis* (as *Z. chilensis*) to group as the sister taxon to *D. nasutus* (as *Z. nasuta* [Müller & Henle 1841]), with *D. chilensis* (as *Z. flavirostris*) from the Falkland Islands as their sister taxon. In combination, these results suggest that closer examination of these skates from Chile and the Falkland Islands is in order.

Here we report on the results of morphological and additional molecular work comparing new specimens from Chile and the Falkland Islands. This work confirms that the specimens from these two regions represent different species. Given the brevity of the original description, and lack of type material of *D. chilensis*, a newly collected specimen from near the type locality in Chile is designated as a neotype, and this species is redescribed. The form from the Falkland Islands is formally described as a new species. *Zearaja* is synonymized with *Dipturus* to reflect the phylogenetic relationships among *Dipturus* species and morphological and molecular data supporting these relationships are presented. The diagnosis of the latter is revised accordingly.

Materials and methods

In total, 50 specimens (30 males and 20 females) of *Dipturus chilensis*, ranging from 56 cm to 96 cm in total length (TL), were collected for this study from artisanal fisheries from the Chilean coast. Three of these specimens, two mature males and one mature female, were retained and deposited at the National Museum of Natural History of Santiago, Chile (MNHNCL) for further examination, one of the mature males was designated as the neotype for *D. chilensis*. Additionally, a total of 41 specimens (12 males and 29 females) of *Dipturus lamillai* **sp. nov.**, ranging from 48.5 cm to 114 cm in TL, was collected from two research cruises conducted by the Fisheries Department of the Falkland Islands in 2013 and 2016. Three skates, two mature males and one mature female, were retained as type specimens. An adult male (holotype) and an adult female (paratype) were deposited at MNHNCL; another adult male (paratype) was deposited at the California Academy of Sciences, San Francisco, USA (CAS). The geographic localities from which the voucher and type specimens of both species were collected are depicted in Fig. 1, along with the localities of the nine specimens of *D. chilensis* and five other specimens of *D. lamillai* **sp. nov.** for which NADH2 sequence data were generated de novo (Table 1). Additional information for all skate specimens collected in this study from Chile and the Falkland Islands can be accessed in the Global Cestode Database (GCD) (elasmobranchs.tapewormdb.uconn.edu) by entering CHL or FA in the Collection Code field, and the specimen number of interest in the Collection Number field.

Morphological methods. For the purpose of this study, specimens were retained after capture to be measured and photographed while still fresh. Individuals chosen as type and voucher specimens to be deposited in collections were frozen as soon as possible after capture. These specimens were subsequently thawed, fixed in sea water buffered formaline (9:1), and transferred to ethanol (70%). Measurements taken were based on Last *et al*. (2008), as modified by Concha *et al.* (2016). Measurements are presented as a percentage of TL (Table 2); data for voucher and paratype specimens are provided in parentheses (male; female). Radiographs (38 kV; 41 MAs) were used to count vertebrae and radials of the left pectoral and pelvic fin from the neotype of *D. chilensis,* and the holotype and female paratype of *D. lamillai* **sp. nov.** Tooth counts are provided for the neotype and voucher specimens retained for the redescription of *D. chilensis* and for type specimens for the description of *D. lamillai* **sp. nov.**

Molecular methods. Tissue samples of about 10 mm^3 from the liver of each specimen for which sequence data were generated were preserved in ethanol (95%). In total, sequence data for 1,043 base pairs (bp) of the NADH2 gene were generated for the neotype (CHL-88) and 10 voucher specimens (CHL-76, CHL-79, CHL-89, CHL-90, CHL-97, CHL-98, CHL-104, CHL-170, CHL-171, CHL-172) of *Dipturus chilensis* collected off the coast of Chile

as well as for the holotype (FA-46), two paratypes (FA-39, FA-47), and five voucher specimens (FA-1, FA-3, FA-8, FA-9, FA-10) of *D. lamillai* **sp. nov.** from the Falkland Islands. For comparative purposes, data were also generated for three specimens of *D. nasutus* (ZN-1, ZN-5, ZN-6) from New Zealand, obtained from the Auckland Museum (Accession Nos. MA37720, MA37717, and MA37715, respectively), and one specimen each of *D. pullopunctatus* (Smith 1964) (AF-9) from South Africa and *D. oxyrinchus* (Linnaeus, 1758) (AZ-10) from the Azores. Based on the phylogenetic tree presented by Naylor *et al.* (2012b), data were also generated for one specimen each of *Okamejei hollandi* (Jordan & Richardson 1909) (KA-340) and *O. cairae* Last, Fahmi & Ishihara 2010 (KA-330) obtained from a fish market in Pontianak, West Kalimantan, Indonesian Borneo, and one specimen of *O. kenojei* (Müller & Henle 1841) (JP-2) obtained from a local fisherman in Yokohama, Kanagawa Prefecture, Japan. Sequence data for all 27 specimens were submitted to GenBank; accession numbers are included in Table 1. For comparative purposes, sequence data for NADH2 were extracted from the mitochondrial genomes available in GenBank for two specimens identified as *Z. chilensis* (i.e., KF648508 and KJ913073).

DNA was extracted using DNeasy Blood & Tissue Kit (QIAGEN), following the kit protocol, and was quantified using a NanoDrop 2000 micro-volume spectrophotometer (Thermo Fisher Scientific, Waltham, MA). Extracted DNA samples were diluted to a concentration of 50 ng/µl. Polymerase chain reaction (PCR) was used to amplify the NADH2 gene. PCR reactions were carried out in a 10.0 µl reaction, containing 1 µl of DNA template, 5.0 µl of GoTaq Green 2x Master Mix (Promega), 2.0 µl water (molecular grade), 0.25 µl of each of the forward (10µM) and reverse (10µM) primers. The following primers were used in different combinations for both the PCR amplification and cycle sequencing: ILEM (5'- AAGGAGCAGTTTGATAGAGT- 3') and ASNM (5'-AACGCTTAGCTGTTAATTAA-3') (Naylor *et al.* 2005); and ILEM_SeqF (5'- AAGCTTTTGGGCCCATACC-3') and ASNM_SeqR (5'-AAGCTTTGAAGGCTTTTGGT-3'), which were developed by E. Jockusch for this study.

Amplification of the NADH2 gene was done using the S1000 thermal cycler (Bio-Rad Laboratories, Inc., Philadelphia, PA) with a touchdown cycling protocol as follows: one cycle of denaturation at 96°C for 4 minutes and for 30 seconds, followed by 12 cycles of annealing (-1°C at each cycle) starting at 60°C for 30 seconds, and extension starting at 72°C for 1 minute and 96°C for 30 seconds; then 30 cycles starting at 96°C for 30 seconds, 48°C for 30 seconds, and 72°C for 1 minute; and a final cycle at 72°C for 2 minutes and 4°C for 3 minutes. We verified successful amplification of the NADH2 gene by running 2 µl of the PCR product on a 1% agarose gel with SYBR-SAFE genomic DNA stain (Thermo Fisher Scientific) in 1x TBE buffer. Removal of PCR primers and excess dNTPs was done by adding 0.1 µl of Exonuclease I (20U/µl) (New England Bio Labs, Ipswich, MA) and 0.4 µl of FastAP (Thermo Fisher Scientific) (1U/µl) and 1 µl of water (molecular grade) to 8 µl of each PCR product. The PCR and enzyme mix was then incubated at 37°C for 30 minutes followed by an enzyme deactivation step at 80°C for 20 minutes.

Cleaned PCR products were then used as a template for cycle sequencing. The cycle sequencing PCR consisted of the following reagents in a final volume of 8.5 µl: 2.1 µl of molecular grade water, 3.2 µl of either the forward or reverse sequencing primer (1 µM), 1.75 µl of cleaned PCR product, and 1.2 µl 5x Sequencing Buffer and 0.25 µl BigDye v1.1 or v3.1 Terminator mix (Thermo Fisher Scientific). The thermal cycling protocol specified an initial denaturation of 3 minutes at 96°C followed by 47 cycles of denaturation for 30 seconds at 96°C; annealing for 30 seconds at 50°C and extension for 4 minutes at 60°C. Cycle sequencing products were then cleaned with 650 µl of hydrated Sephadex G-50 Fine beads (3.1 g Sephadex: 50 ml D.I. water) (Sigma-Aldrich, St. Louis, MI) for each sequencing reaction. Sequencing of both strands was carried out on an ABI 3130xl Genetic Analyzer with a 50 cm capillary array (Applied Biosystems, Foster City, CA). Contigs were assembled and sequences were manually edited using Geneious 8.1.7 (Biomatters Ltd., Auckland, New Zealand).

Molecular analyses. All sequences were trimmed to 1,043 bp in length. Sequence differences, both within and among species, were estimated using p-distance (Jukes & Cantor 1969) as implemented in Geneious (v. 8.1.7). Neighbor-Joining analysis, also implemented in Geneious (v. 8.1.7), using the Jukes-Cantor genetic distance model and *O. kenojei* as the outgroup species, was used to generate a tree for examining specific identities (Fig. 13). We would emphasize that, given this is not a phylogenetic method, the topology of the resulting tree should not be interpreted to represent phylogenetic relationships.

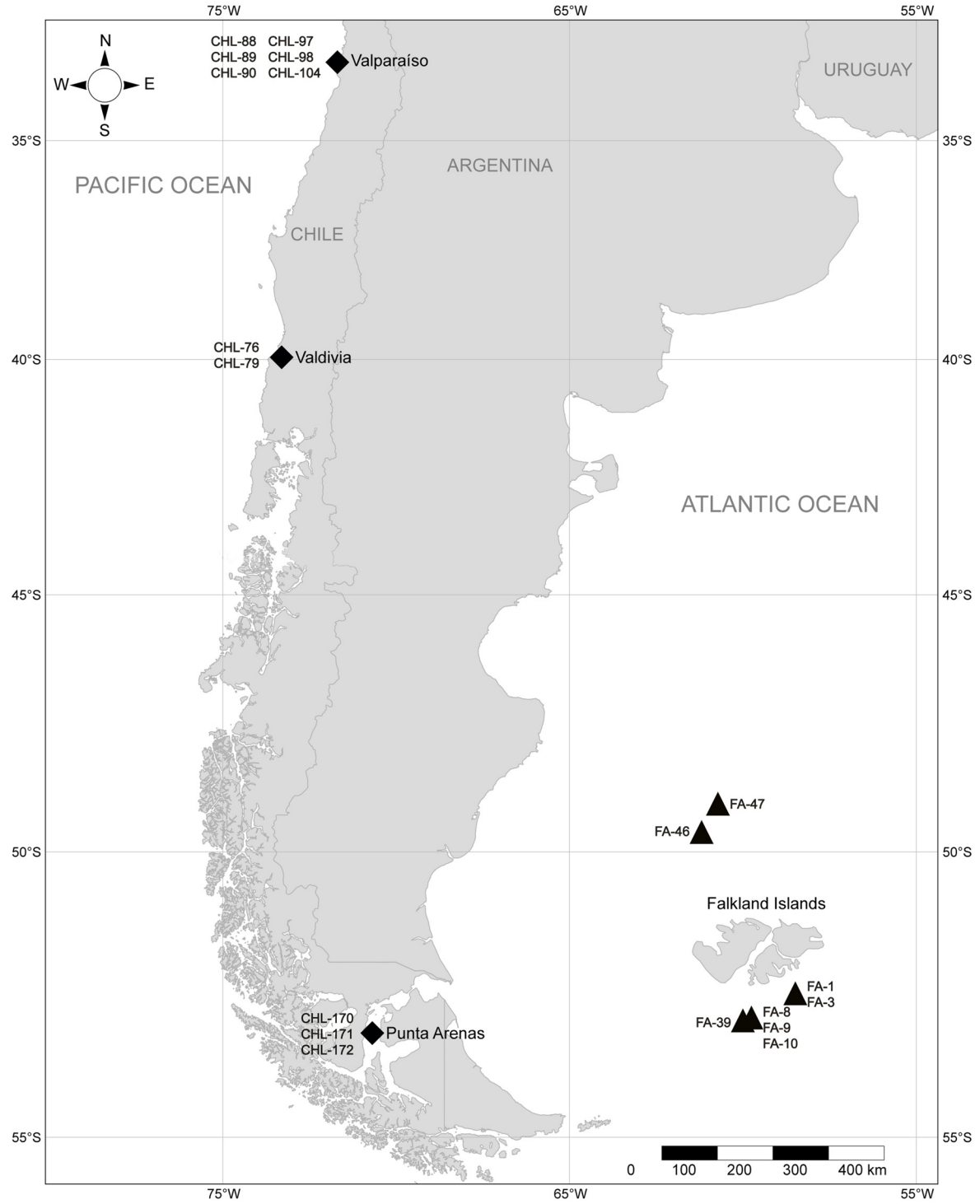

FIGURE 1. Map showing geographic locations of specimens of *Dipturus chilensis* (diamonds) and *D. lamillai* **sp. nov.** (triangles) for which NADH2 sequence data were generated.

TABLE 1. Type and voucher specimens used in the molecular analysis.

Species	Sex	Type status	Col. No.	Museum No.	GenBank No.
Dipturus chilensis	Male	Voucher	CHL-76	N/A	MK613956
Dipturus chilensis	Male	Voucher	CHL-79	N/A	MK613957
Dipturus chilensis	Male	Neotype	CHL-88	MNHNCL ICT 7549	MK613955
Dipturus chilensis	Female	Voucher	CHL-89	MNHNCL ICT 7550	MK613958
Dipturus chilensis	Female	Voucher	CHL-90	N/A	MK613959
Dipturus chilensis	Male	Voucher	CHL-97	N/A	MK613960
Dipturus chilensis	Male	Voucher	CHL-98	N/A	MK613961
Dipturus chilensis	Male	Voucher	CHL-104	N/A	MK613962
Dipturus chilensis	Male	Voucher	CHL-170	N/A	MK613963
Dipturus chilensis	Female	Voucher	CHL-171	N/A	MK613964
Dipturus chilensis	Male	Voucher	CHL-172	N/A	MK613965
Dipturus chilensis	N/A	Voucher	N/A	N/A	KJ913073*
Dipturus lamillai **sp. nov.**	Female	Voucher	FA-1	N/A	MK613969
Dipturus lamillai **sp. nov.**	Female	Voucher	FA-3	N/A	MK613970
Dipturus lamillai **sp. nov.**	Male	Voucher	FA-8	N/A	MK613971
Dipturus lamillai **sp. nov.**	Female	Voucher	FA-9	N/A	MK613972
Dipturus lamillai **sp. nov.**	Male	Voucher	FA-10	N/A	MK613973
Dipturus lamillai **sp. nov.**	Male	Paratype	FA-39	CAS 242403	MK613967
Dipturus lamillai **sp. nov.**	Male	Holotype	FA-46	MNHNCL ICT 7531	MK613966
Dipturus lamillai **sp. nov.**	Female	Paratype	FA-47	MNHNCL ICT 7532	MK613968
Dipturus lamillai **sp. nov.**	N/A	Voucher	N/A	N/A	KF648508*
Dipturus nasutus	Female	Voucher	ZN-1	MA37720	MK613974
Dipturus nasutus	Male	Voucher	ZN-5	MA37717	MK613975
Dipturus nasutus	Female	Voucher	ZN-6	MA37715	MK613976
Dipturus oxyrinchus	Male	Voucher	AZ-10	N/A	MK613977
Dipturus pullopunctatus	Female	Voucher	AF-9	N/A	MK613978
Okamejei cairae	Female	Voucher	KA-330	H 7099-01	MK613979
Okamejei hollandi	Female	Voucher	KA-340	N/A	MK613980
Okamejei kenojei	Female	Voucher	JP-2	N/A	MK613981

*Specimens for which sequence data were obtained from GenBank.

Results

Family Rajidae

Dipturus Rafinesque 1810

Type Species: *Raja batis* Linnaeus 1758 by original designation.
Synonyms: *Raja* (*Dipturus*) as subgenus by Stehmann (1970); *Zearaja* Whitley 1939.

Diagnostic features. Modified from Ishihara (1987), Leible (1987), McEachran & Dunn (1998), and Last *et al*.

(2016). Disc broad, rhombic-shaped, outer corners sharply rounded to angular; margins deeply concave anteriorly and produced posteriorly; brownish to dark grey on both dorsal and ventral surfaces; with numerous mucus and sensory pores of irregular pattern visible as black dots and short streaks, mostly on ventral surface; snout elongated, acutely angled, with slightly translucent area flanking rostral cartilage; rostral cartilage long, its length from tip to axils of nasal capsules usually more than 60% of dorsal head length; rostral appendices attached over all or most of length to rostral cartilage; pre-cerebral fontanelle elongated, narrow, extending anteriorly into the rostral cartilage well anterior to leading edge of nasal capsules; nasal capsules without basal fenestrae; inter-nasal plate broad; inter-narial width usually exceeding 60% of pre-nasal length; pre-orbital processes developed; scapulocoracoid without anterior bridge; distance between pro- and meso- less than distance between meso- and meta-condyles, with post-ventral fenestra; propterygium of pectoral girdle falling short of middle length of rostral shaft; claspers enlarged, broad at shield, with pointed or spatulated distal lobe; shield long or short, capable of rotation; clasper glans expanded, with cleft, sentina, pseudorhipidion, and rhipidion; spike concealed by integument or exposed; shield with pleated lamellae on its inner surface; sentinel may be absent; funnel absent; clasper skeleton with 3 dorsal terminal cartilages on dorsal aspect of clasper; 1 or 2 accessory terminal cartilages; pectoral radials 77–86; trunk vertebrae 25–34, pre-dorsal caudal vertebrae 52–64; tail with two subterminal dorsal fins; caudal fin small to rudimentary; electrocytes in caudal electric organs with cortical processes; egg capsules broad, convex dorsally, concave or flattened ventrally, short horns, length of egg capsule excluding horns, more than 65 mm, with lateral keels and posterior apron.

Remarks. The genus *Dipturus* was established by Rafinesque (1810; page 16) as: "Due ale dorsali sopra la coda, nessun ala caudale alla sua estremità—Oss. La *Raja Batio* di Linneo compone sola questo genere" ("Two dorsal fins on the tail, without a caudal fin at the extremity—the *Raja Batio* of Linnaeus is the only one composing this genus"). Despite its brevity and lack of detail, the diagnosis has been widely accepted and, according to Last *et al.* (2016), the genus now comprises 38 species. However, molecular work suggests that the monophyly of *Dipturus* is compromised by the recognition of *Zearaja* as a valid genus because the latter constitutes a small clade deeply nested within a clade of *Dipturus* species (e.g., Naylor *et al.* 2012b; Vargas-Caro *et al.* 2016b). The genus *Zearaja* was established by Whitley (1939; page 254) for *Z. nasuta*. Beyond noting that the species "has produced snout, shouldered pectorals, surface of disc rough above and with blackish pits below. A median row of strong spines along tail, one on middle of back, and a few near the eyes", Whitley (1939) provided no diagnosis. Despite this, *Zearaja* was recognized at the subgeneric rank by Last & Yearsley (2002) and was subsequently returned to generic status by Last & Gledhill (2007). The latter authors provided a diagnosis and considered this genus to also include the Maugean skate (*Z. maugeana* Last & Gledhill 2007), the New Zealand Rough-skate (*Z. nasuta*), and the Yellow-nose skate (*Z. chilensis*). Additionally, Gabbanelli *et al*. (2018) resurrected *Raja brevicaudata* Marini 1933 from Argentinean waters, and tentatively transferred this species to the genus *Zearaja* based largely on clasper anatomy.

The most compelling morphological feature presented by Last & Gledhill (2007) that both unites members of *Zearaja* and distinguishes them from species of *Dipturus* is their relatively simple clasper morphology. Compared with *Dipturus*, the claspers of *Zearaja* have shorter ventral terminal and dorsal terminal 2 cartilages, a spatulated distal lobe, lack both accessory terminal cartilage 1 and the sentinel, and they represent 24–32% of total length. However, Ebert *et al*. (2008) reported claspers of *D. campbelli* (Wallace 1967), *D. pullopunctatus*, and *D. springeri* (Wallace 1967) to range between 20% and 32% of total length. Furthermore, Last & Gledhill (2007) included several additional details of clasper morphology in their diagnosis of *Zearaja* that are also present in some species of *Dipturus*. For instance, a spatulate distal end of the axial cartilage in *Zearaja* was also reported in *D. pullopunctatus* and *D. lanceorostratus* (Wallace 1967) by Hulley (1970; 1972). Moreover, Hulley (1972) highlighted the absence of a sentinel in *D. pullopunctatus*, despite the presence of an accessory terminal 1 cartilage. Finally, although not necessarily of generic importance, the eurybathic depth range of *Zearaja* overlaps with at least 17 species of *Dipturus* (see Last *et al*. 2016).

Given the otherwise substantial morphological similarity between the two genera, these results suggest that the simple clasper morphology seen in species assigned to *Zearaja* unites a subset of *Dipturus* species but does not justify recognition of *Zearaja* as a genus independent of *Dipturus* if the monophyly of the latter genus is to be maintained. As a consequence, *Zearaja* is here considered a junior synonym of *Dipturus*. In terms of the species assigned to the genus by Last & Gledhill (2007), Last *et al*. (2016), and Gabbanelli *et al*. (2018), following McEachran & Dunn (1998), *D. nasutus* and *D. chilensis* are considered members of *Dipturus* and *D. maugeanus*

(Last & Gledhill, 2007) **n. comb.**, *D. argentinensis* (Díaz de Astarloa, Mabragaña, Hanner & Figueroa 2008) **n. comb.**, and *D. brevicaudatus* (Marini 1933) **n. comb.** are hereby transferred to that genus.

***Dipturus chilensis* (Guichenot 1848)**
Yellow-nose skate, raya volantín
Type locality: Quintero, Valparaíso, Central Chile.
(Figures 2–6; 12A–B; Table 2)

Neotype. Mature male MNHNCL ICT 7549, tissue voucher No. CHL-88, 90.7 cm TL, collected with a gillnet in Valparaíso Bay, central Chile, southeastern Pacific Ocean (32°53'22.94"S, 71°31'32.16"W; approx. 40 m) on January 8th, 2014 by Veronica Bueno and Francisco Concha.

Voucher specimens. A total of 49 specimens was collected and observed. Two specimens were kept in the ichthyological collection of the Chilean Museum of Natural History (MNHNCL ICT) in Santiago, Chile: a mature male (MNHNCL ICT 7569; CHL-138), 94.9 cm TL, collected with a bottom longline near Puerto Gala, Aysén, inner waters of Chilean Patagonia, southeastern Pacific Ocean (44°15'30.89"S, 73°12'39.97"W; approximately 400 m), on October 24th, 2016 by Erwin Pacheco; a mature female MNHNCL ICT 7550, tissue voucher No. CHL-89, 73.5 cm TL, collected with a gillnet off Valparaíso, central Chile, southeastern Pacific Ocean (32°53'22.94"S, 71°31'32.16"W; approx. 40 m), on January 8th, 2014 by Veronica Bueno and Francisco Concha.

Specimens sequenced. Sequence data for NADH2 were generated for the neotype and 10 additional specimens of *D. chilensis*. Information on sex, type status, collection number (GCD), and accession numbers for museum and GenBank for each of the specimens is provided in Table 1.

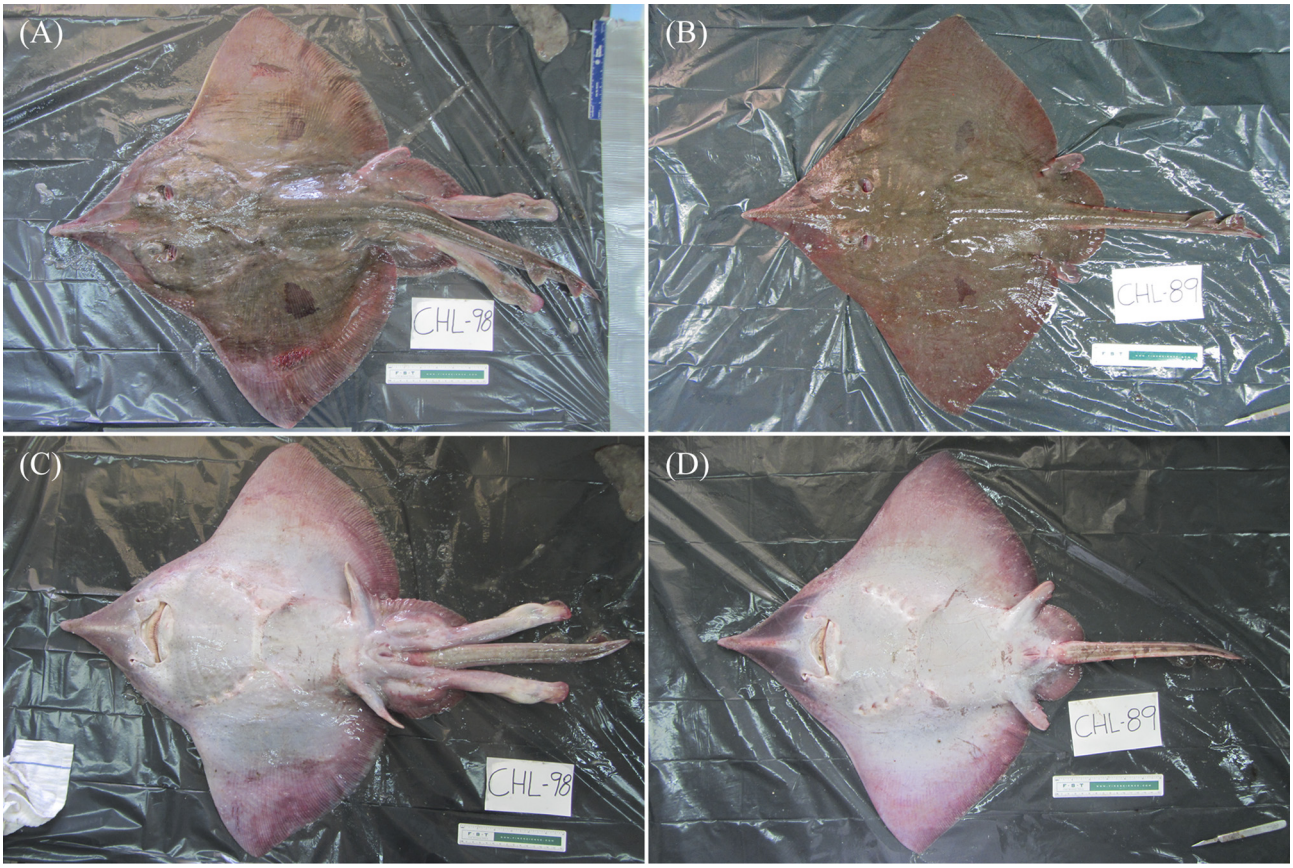

FIGURE 2. Adult specimens of *Dipturus chilensis*: (A, C) Dorsal and ventral views of male (CHL-98), respectively. (B, D) Dorsal and ventral view of female voucher (MNHNCL ICT 7550; CHL-89), respectively. Scale-ruler: 15 cm.

Diagnosis. A medium-sized species of *Dipturus*, up to at least 118.0 cm TL (CHL-85). It is distinguishable from its congeners by the following combination of characters: When fresh, dorsal surface of body plain brownish to greyish, with some lighter small spots randomly distributed dorsally; one red to purple ocellus over center of

each pectoral fin. When fresh, ocelli with well-defined margins, irregular in shape, usually indistinguishable in fixed specimens; ventrally, white to grey with lighter patches over area of gill openings and beneath mouth; area flanking rostral cartilage membranous and slightly translucent when fresh, opaque and yellowish when fixed; disc relatively broad with angular apices, width 76.4 (75.0; 77.0) % TL; snout relatively short and broad. Tail longer in males (42.2 [40.8] % TL) than in female voucher ([38.8] % TL). Ventral head length 35.1 (34.2; 37.7) % TL; pre-orbital snout length 2.4 (2.9; 2.9) times distance between orbits; orbit diameter 0.5 (0.5; 0.6) of inter-orbital width. Dorsal surface of disc and tail in males with central longitudinal band of dermal denticles extending from anterior margin of rostral cartilage to tail, including anterior margins of dorsal and caudal fins; thin band of dermal denticles at anterior margins of pectoral fins, extending from anterior fontanelle to front line of alar thorn patches. Dorsal surface of disc and tail of females covered with small dermal denticles, except for external margins of pectoral fins, pelvic fins, and area surrounding caudo-central thorns. Orbital thorns present; single nuchal thorn often absent; both sexes lacking scapular thorns; patch of malar thorns only in adult males; alar thorns only in adult males; medial-dorsal and lateral-dorsal thorns may be present in large specimens, especially in large females (e.g., CHL-90). Small central-caudal thorns mostly arranged in longitudinal pairs in males and females, additional two longitudinal rows of fine, sharp and posteriorly oriented lateral-caudal thorns may be present in large specimens. Ventral sensory pores small, distinct, black-edged, most abundant on snout and around mouth, scattered over area between gill openings, sparsely spaced on abdominal area and pectoral fins.

Redescription. Morphometric and meristic data are provided for the neotype (mature male, CHL-88) and two vouchers (one mature male and one mature female, CHL-138 and CHL-89, respectively), and are expressed as CHL-88 (CHL-138; CHL-89). Redescription came from fixed and fresh specimens of both sexes unless otherwise indicated. Much of dorsal surface plain light brown to dark grey; some specimens with small, scattered light brownish spots dispersed over dorsal surface of disc (Fig. 2A–B); light yellowish-brown coloration or slightly translucent adjacent to rostral cartilage and anterior fontanelle, contrasting with darker area on rostral cartilage (Fig. 3A–B). Single irregularly shaped red to purple ocellus with solid margins over center of pectoral fins, conspicuous in fresh specimens, lighter to undetectable in fixed specimens. Anterior margin of pelvic fins whitish. Outer posterior margin of spiracle, base of spiracular pseudo-branch, and area inside spiracle, white (Fig. 3A–B).

FIGURE 3. Adult specimens of *Dipturus chilensis*: (A, C) Dorsal view of head and oro-nasal area, respectively, of male neotype (MNHNCL ICT 7549; CHL-88). (B, D) Dorsal view of head and oro-nasal area, respectively, of female voucher (MNHNCL ICT 7550; CHL-89).

Ventral surface light grey or whitish to dark brown in center of disc extending to inner half of pectoral fins; darker areas on ventral side of disc mostly restricted to oro-nasal area, inter-branchial space and abdomen, light brown to whitish outer margins, except for posterior margins of pectoral fins, which are brownish (Fig. 2C–D); white irregular patches, more conspicuous in fixed specimens, posterior to mouth, gill openings, base of tail, and ventral surface of claspers.

Disc rhomboidal, 1.3 (1.2; 1.2) times broad as long; snout angle in front of spiracles 79.2 (71.7; 75.2) degrees; axis of greatest width at 64.1 (58.3; 63.9) % of TL; anterior margin of disc concave anteriorly, convex anterior-laterally to eyes, strongly or moderately concave behind line of spiracles in males and females; apex narrowly rounded to sub-angular; posterior margin convex; free rear tip very broadly rounded.

Head elongated, snout narrowly pointed, rigid, pre-orbital snout length 5.0 (6.1; 5.0) times orbit length, 2.4 (2.9; 2.9) times distance between orbits; pre-upper jaw length 1.4 (1.7; 1.9) times distance between nostrils. Orbit small, diameter 0.5 (0.5; 0.6) times distance between orbits. Spiracles 0.8 (0.8; 0.8) times orbit diameter; spiracle opening oval. Nostrils semi-circular, with nearly straight inner margins; anterior nasal flap expanded, not overlapping nostril; anterior margin of nostril flap weakly lobed, partly concealed beneath nasal curtain, posterior inner margin not or barely concealed beneath nasal curtain. Posterior lobes of nostrils forming well developed nasal curtain, produced slightly postero-laterally, slightly concave external margins, with fringed posterior margins, shorter in males than in females, reaching first series of teeth in male neotype, covering whole upper mandible in female voucher (Fig. 3C–D). Distance between nostrils 2.1 (2.0; 2.1) distance between first gill slits, 1.2 (1.8; 1.2) distance between fifth gill slits. Upper jaw more arched in males than in female, indented at symphysis; lower jaw convex in both sexes. Teeth uni-cuspid, with sub-circular bases, arranged in longitudinal rows; cusps of medial teeth long, sub-conical, pointed, posteriorly and lingually directed in upper and lower jaws; cusps of lateral teeth shorter and slightly oblique; cusps of all teeth in mature males narrower and longer than in females (Fig. 3C–D).

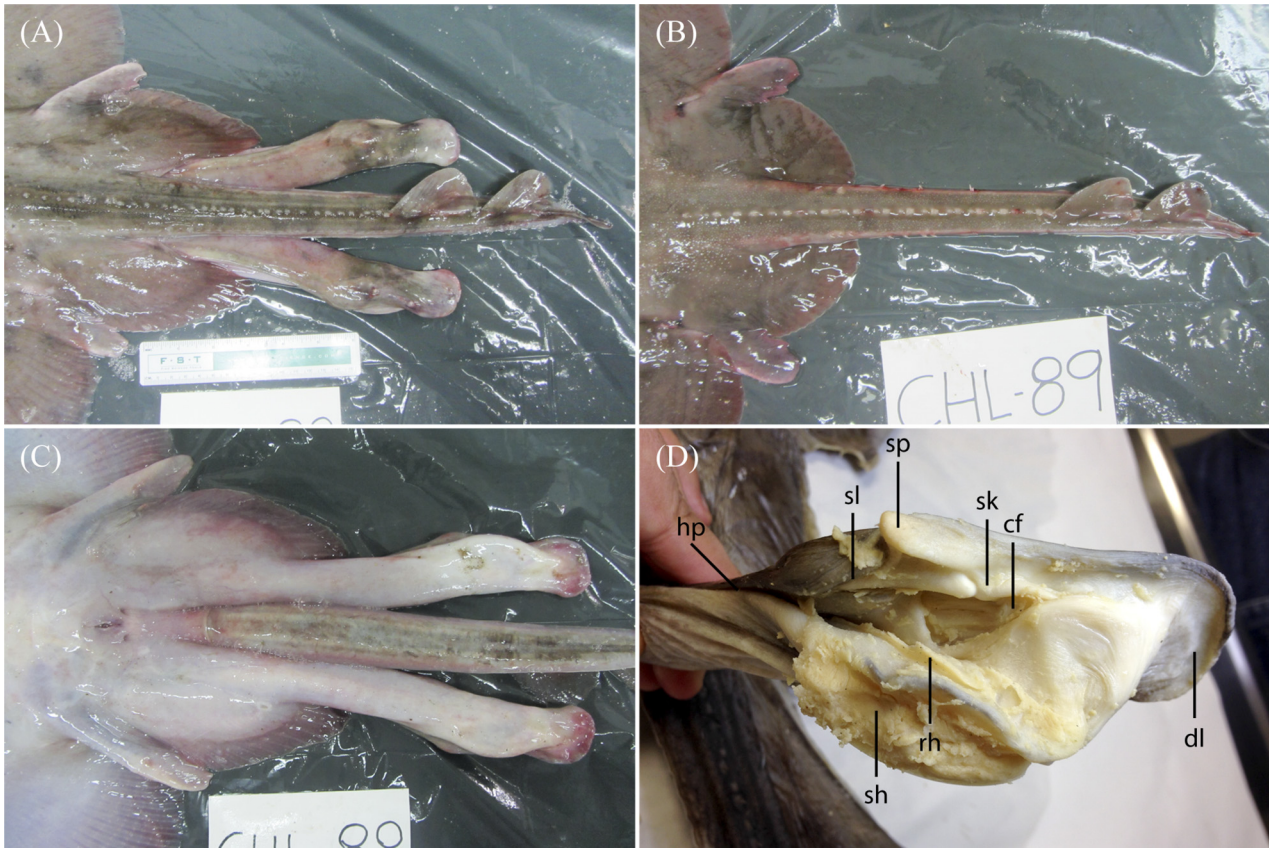

FIGURE 4. Adult specimens of *Dipturus chilensis*: (A) Dorsal view of tail of male neotype (MNHNCL ICT 7549; CHL-88). (B) Dorsal view of tail of female voucher (MNHNCL ICT 7550; CHL-89). (C) Ventral view of of male neotype (MNHNCL ICT 7549; CHL-88). (D) Internal components of right clasper, lateral view. cf—cleft, dl—distal lobe, hp—hypopyle, rh—rhipidion, sh—shield, sl—slit, sk—spike, and sp—spur.

Pelvic fins of medium size, deeply forked (Fig. 4A–B); anterior lobe relatively short, slender, bluntly pointed distally, 0.6 (0.6; 0.8) times length of posterior lobe, lateral margin entire, inner margin incised; posterior margin of distal pelvic lobe moderately elongate in males, rounded in females, longer in mature males than in females, 20.3

(18.5; 16.9) % of TL. Claspers elongate, 30.7 (31.0) % of TL, moderately broadened at shield, dorsoventrally depressed at distal lobe, lacking dermal denticles; apopyle and hypopyle distinguishable as narrow slits in external lateral view. Internal components: cleft, shield, slit, spike, spur, and rhipidion; dermal denticles absent (Fig. 4D).

Tail relatively short, length from rear of cloaca to tail tip 0.7 (0.7; 0.6) times distance from tip of snout to rear of cloaca. Tail narrowing posteriorly, width at pelvic fin axils 1.1 (1.2; 1.4) times width at mid-length, 1.4 (1.6; 1.4) times width at first dorsal fin origin, 1.2 (1.4; 1.4) times height at pelvic fin axils, 2.0 (1.6; 1.9) times height at mid-length, 1.5 (1.4; 1.6) times height at first dorsal fin origin. Tail in males flattened dorsally, convex ventrally at base, becoming depressed and oval medially, triangular between dorsal fins, ventral face almost flat; in females, more uniformly depressed along its length, moderately flattened dorsally, convex ventrally at the base, oval at mid-length, triangular with a more flattened base between dorsal fins. Lateral tail fold narrow, relatively long, originating as a low membranous ridge beside or slightly posterior to pelvic axil, extending sub-terminally to tail tip, not obviously broader at any point along its length, maximum width about half caudal fin height in neotype, about as wide as caudal fin height in female voucher.

Dorsal fins sub-equal in size, similar in shape, apices broadly rounded, not fringed (Fig. 5A–B), posterior margins shorter than anterior margins, free rear tip broadly rounded. First dorsal fin long and weakly convex, slightly taller and more upright than second; first dorsal fin height 1.7 (1.3; 1.8) in base length. Second dorsal-fin base shorter in males, subequal or only marginally shorter than first dorsal fin base in female voucher; inter-dorsal space moderate (Fig. 5A–B), rear tip of first dorsal fin not overlapping base of second; distance from first dorsal fin origin to tail tip 2.7 (2.9; 2.7) times first dorsal fin base length, 3.6 (3.8; 3.9) times caudal fin length; first dorsal fin base length 1.3 (1.3; 1.4) times caudal fin length. Epichordal caudal fin lobe developed; base long, maximum height 0.1 (0.2; 0.1) times base length, relatively uniform in height along its length, dorsal margin weakly convex, connected sub-basally to second dorsal fin; hypochordal caudal lobe absent.

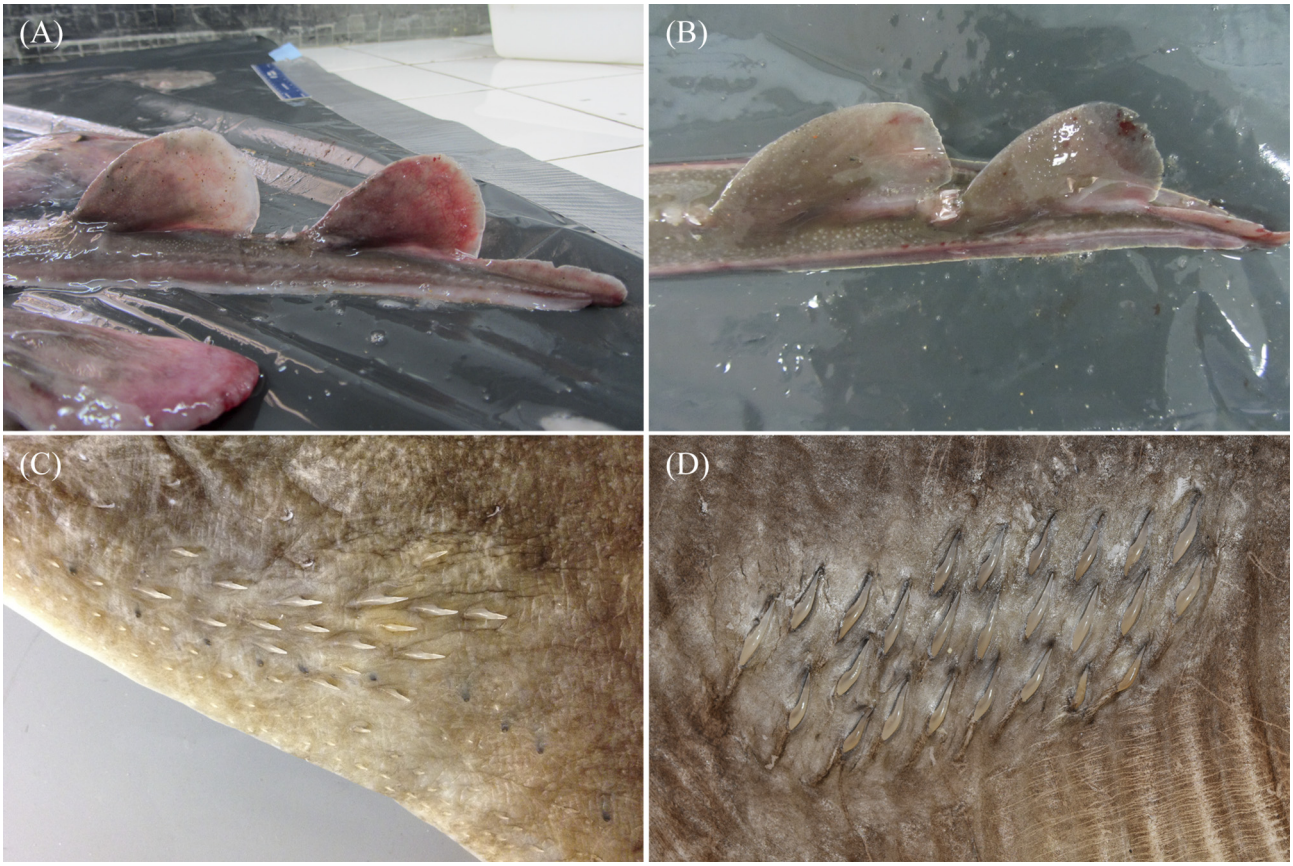

FIGURE 5. Adult specimens of *Dipturus chilensis*: (A) Dorsal and caudal fins adult male (CHL-98). (B) Dorsal and caudal fins of female voucher (MNHNCL ICT 7550; CHL-89). (C) Left malar thorns of male neotype (MNHNCL ICT 7549; CHL-88). (D) Left alar thorns of adult male voucher (MNHNCL ICT 7569; CHL-138).

Orbital thorns variable in size and number, with rounded or oval base; in males 6 thorns on each orbit, 2 on pre-orbit, 3 on mid-orbit, and 1 on post-orbit; in female voucher specimen 4 on pre-orbit, 2 on mid-orbit, 2 on post-orbit; anterior and posterior orbital thorns flanked by dermal denticle patches (Figs. 3A–B; 12A–B). Distribution pattern and presence of other thorns on disc and tail differ considerably between sexes and may vary within sexes. Malar and alar thorns present only in males; malar thorns (Fig. 5C) 18 (6), posteriorly directed, very sharp, not embedded; alar thorns (Fig. 5D) 23 (25), medially posterior-directed, some embedded, longer than malar and caudal thorns, with very sharp tips. Single nucal thorn and scattered rostral thorns present or absent in both sexes; scapular thorns absent in both sexes. Single row of approximately 10 medial-dorsal thorns in females of large sizes (e.g., CHL-90), scattered and continuous with central row of caudal thorns. Lateral-dorsal row of about 12 acutely pointed thorns in large females, may extend posteriorly to become one of lateral row of caudal thorns. Males with 3 rows of caudal thorns; central row of thorns 30 (23) (Fig. 4A–B), posteriorly directed, extending in linear series, mostly in pairs, beginning posteriorly to pelvic girdle and extending to first dorsal fin; about 6 widely spaced lateral-caudal thorns on each side of central row from behind the pelvic axil. Female voucher specimen (CHL-89) with 3 rows of caudal thorns; central row of 31 thorns to first dorsal fin; lateral rows of 7 posteriorly directed thorns. Additional rows of lateral-caudal thorns may be present in large specimens, merging posteriorly to pelvic fin axils, above lateral tail fold and beneath upper lateral caudal row, and extend to second dorsal fin (e.g. CHL-90); inter-dorsal thorns 3 (2; 3), not aligned, posteriorly directed, sharp.

Distribution pattern and abundance of dermal denticles on dorsal surface of disc and tail sexually dimorphic (Fig. 12A–B). In males, denticles small and sparse, except in anterior portion of rostrum, where large and small denticles occur; dense, narrow denticle band along antero-lateral margin of disc, beginning well anteriorly to malar thorns, reaching to about half of anterior margin of pectoral fin; denticle band covering tip of snout, rostral cartilages, inter-orbital and inter-spiracular spaces, and area behind spiracles; longitudinal patch of denticles along mid-dorsal surface extending to tail tip; on tail mostly flanking central-caudal thorns; fine band of dermal denticles on anterior margin of dorsal fins, sparse over caudal fin; ventral snout and oro-nasal area with scattered, small denticles; dense denticles band beneath rostral cartilage, disc margin to level of about first gill slits, small longitudinal band of flattened and scattered denticles along tail from about posterior margin of pelvic fins. In females, dermal denticles covering most of dorsal surface of disc, pelvic fins, and dorsal and caudal fins on tail; denticles absent only on anterior fontanelle, orbits, spiracles, external margins of disc, and area surrounding caudal-central thorns (Fig. 12A–B). Ventrally, fine dermal denticle bands on anterior margins of disc and scattered over snout; tip of snout more densely covered; small and randomly distributed denticles around cloaca and along tail, not forming defined patches or bands.

Tooth rows (Fig. 3C–D) in upper jaw 42 (45; 36); tooth rows in lower jaw 42 (45; 33). In neotype, pectoral-fin propterygial radials 31, mesopterygial radials 15, metapterygial radials 33, total radials 79; pelvic-fin radials 20; trunk vertebrae 25, pre-dorsal caudal vertebrae 60, vertebrae between origins of dorsal fins 20, total vertebrae about 143.

Egg capsule (Fig. 6) moderate in size, ranging from 9.4 to 14.4 cm in length excluding horns, 6.4 to 7.6 cm in width, barrel shaped, golden brown when fresh, blackish after fixation. Surface smooth with fine longitudinal striations, dorsal surface convex. Anterior horns short, inwardly ventrally curved, not overcrossing; posterior horns moderately long, narrowing posteriorly, not tendril-like. No additional adhesion fibers present. Anterior margin concave, lateral keels present, posterior apron straight, not fringed when recently laid, becoming fringed with time. A more detailed description and observations on oviposition rate can be seen in Concha *et al.* (2012).

Size. Size at hatching and incubation period 17.2 cm TL and 252 days, respectively (Concha *et al*. 2018). Minimum and maximum reported TL 16 and 152 cm, respectively, reported by Fuentealba & Leible (1990) and Licandeo & Cerna (2007), respectively.

Distribution. Known from coastal waters from central Chile to the Strait of Magellan.

Comparisons. The only reported sympatric congener of *D. chilensis* in the southeastern Pacific is the Rough-skin skate, *Dipturus trachydermus*. Adults of the former attain a much smaller size than those of the latter (152 cm versus 257.7 cm, respectively) (Licandeo *et al.* 2006; 2007). The disc of *D. chilensis* is relatively narrower than that of *D. trachydermus* (approx. 72.7% versus 76.0% of TL, respectively) and also darker in coloration (see Krefft & Stehmann 1975). Dorsally, *D. chilensis* is covered with defined patches of small dermal denticles, whereas the dermal denticles of *D. trachydermus* are wider and distributed irregularly throughout the dorsal and ventral surfaces of the body. The dermal denticles on the dorsal surface of the snout of *D. chilensis* are restricted to the

surface of rostral cartilage, while the dermal denticles of *D. trachydermus* also cover the membranous areas flanking the rostral cartilage. The presence of scattered, thick, small dermal denticles throughout the surface of the claspers of *D. trachydermus*, even in sub-adults, contrasts sharply with the smooth claspers of *D. chilensis*. Additionally, the distal lobe of the clasper of *D. trachydermus* is pointed, whereas it is flattened in *D. chilensis*. Six additional species of *Dipturus* have been reported off the coasts of the southwestern Atlantic: *D. argentinensis* (see Díaz de Astarloa *et al*. 2008), *D. bullisi* (see Bigelow & Schroeder 1962), *D. leptocaudus* (see Krefft & Stehmann 1975), *D. mennii* (see Gomes & Paragó 2001), *D. teevani* (see Bigelow & Schroeder 1951), and a taxon previously referred to as *D. chilensis* or *D. flavirostris*, described as *D. lamillai* **sp. nov.** here. *Dipturus chilensis* differs from the first five species in different combinations of characters. The disc of *D. chilensis* is relatively wider than those of *D. argentinensis*, *D. leptocaudus*, and *D. teevani* (i.e., approx. 76.0 versus 74.8, 68.5 and 72.7 % of TL) (Díaz de Astarloa *et al.* 2008; Krefft & Stehmann 1975; Bigelow & Schroeder 1951). The disc of *D. chilensis* is narrower than that of *D. bullisi* (76.0% versus 80.0% of TL) (Bigelow & Schroeder 1962). Whereas the tail of *D. chilensis* narrows posteriorly, in *D. teevani* the tail widens posteriorly (Bigelow & Schroeder 1951). Furthermore, whereas the lateral tail folds are subterminal in *D. chilensis*, they reach only half the length of the caudal fin in *D. teevani*. Additionally, whereas the tail of *D. chilensis* is about 40% of TL, those of *D. argentinensis*, *D. bullisi*, and *D. leptocaudus* are longer (i.e., 47.2, 45.7, and 48 % of TL, respectively) (Díaz de Astarloa *et al.* 2008; Bigelow & Schroeder 1962; Krefft & Stehmann 1975). While the dorsal fins of *D. chilensis* are not connected to one another and thorns are present in the inter-dorsal space, the dorsal fins of *D. teevani* are connected at their bases by a membranous bridge. Scapular thorns are absent in *D. chilensis* but present in *D. mennii* and *D. leptocaudus* (see Gomes & Paragó 2001; Krefft & Stehmann 1975). *Dipturus chilensis* has more than four inter-orbital thorns on each orbit and also has three rows of caudal spines on the tail, whereas *D. bullisi* has only two inter-orbital spines on each orbit and a single row of caudal thorns (Bigelow & Schroeder 1962). Finally, well defined patches of dermal denticles are found throughout much of the dorsal surface of the body of *D. chilensis*, but in *D. argentinensis*, *D. leptocaudus,* and *D. teevani*, dermal denticles are mostly restricted to the dorsal area of the snout (Díaz de Astarloa *et al.* 2008; Krefft & Stehmann 1975; Bigelow & Schroeder 1951).

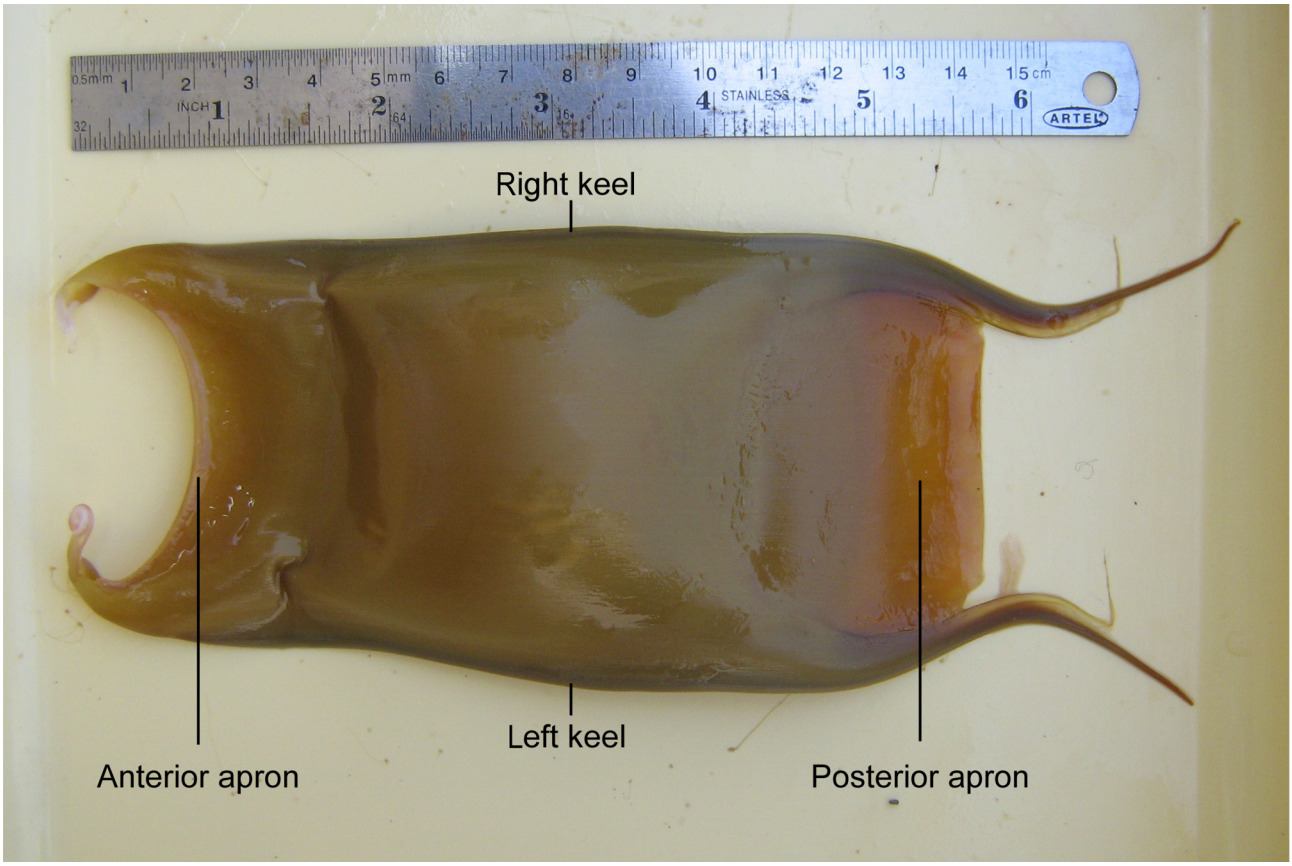

FIGURE 6. Dorsal view of a fresh egg capsule of *Dipturus chilensis* extracted from oviduct of adult female captured in Valparaíso, Chile, close to type locality.

***Dipturus lamillai* sp. nov.**
Warrah skate; raya guará
(Figures 7–11, 12C–D; Table 2)

Holotype. Mature male MNHNCL ICT 7531 (Fig. 7A, C), tissue voucher No. FA-46, 78.7 cm TL, collected with bottom trawl in waters off the Falkland Islands, southwestern Atlantic Ocean (Station 2019; 49.61°S, 61.19°W; 162 m), on February 14th 2016, FV Castelo, cruise ZDLT1-02-2016 Finfish and Rock Cod Biomass Survey, Joost H. W. Pompert.

Paratypes. Two specimens: a mature male (CAS 242403; FA-39), 91.5 cm TL, collected with bottom trawl in waters of the Falkland Islands, southwestern Atlantic Ocean (Station 1271; 53°7.6'S, 60°7.9'W; 515 m), on November 17th 2013, FV Castelo, cruise ZDLT1-11-2013 Skate Biomass and Biological Survey, by Francisco Concha: a mature female (MNHNCL ICT 7532; FA-47) (Fig. 7B, D), 94.2 cm TL, collected with bottom trawl in waters of the Falkland Islands, southwestern Atlantic Ocean (Station 2031; 49.10°S, 60.72°W; 198 m), on February 15th 2016, FV Castelo, cruise ZDLT1-02-2016 Finfish and Rock Cod Biomass Survey, by Joost H. W. Pompert.

Specimens sequenced. Sequence data for NADH2 were generated for the holotype, both paratypes, and five additional specimens of *D. lamillai* **sp. nov.** Information on sex, type status, collection number (GCD), and accession numbers for museum and GenBank of each of the specimens is provided in Table 1.

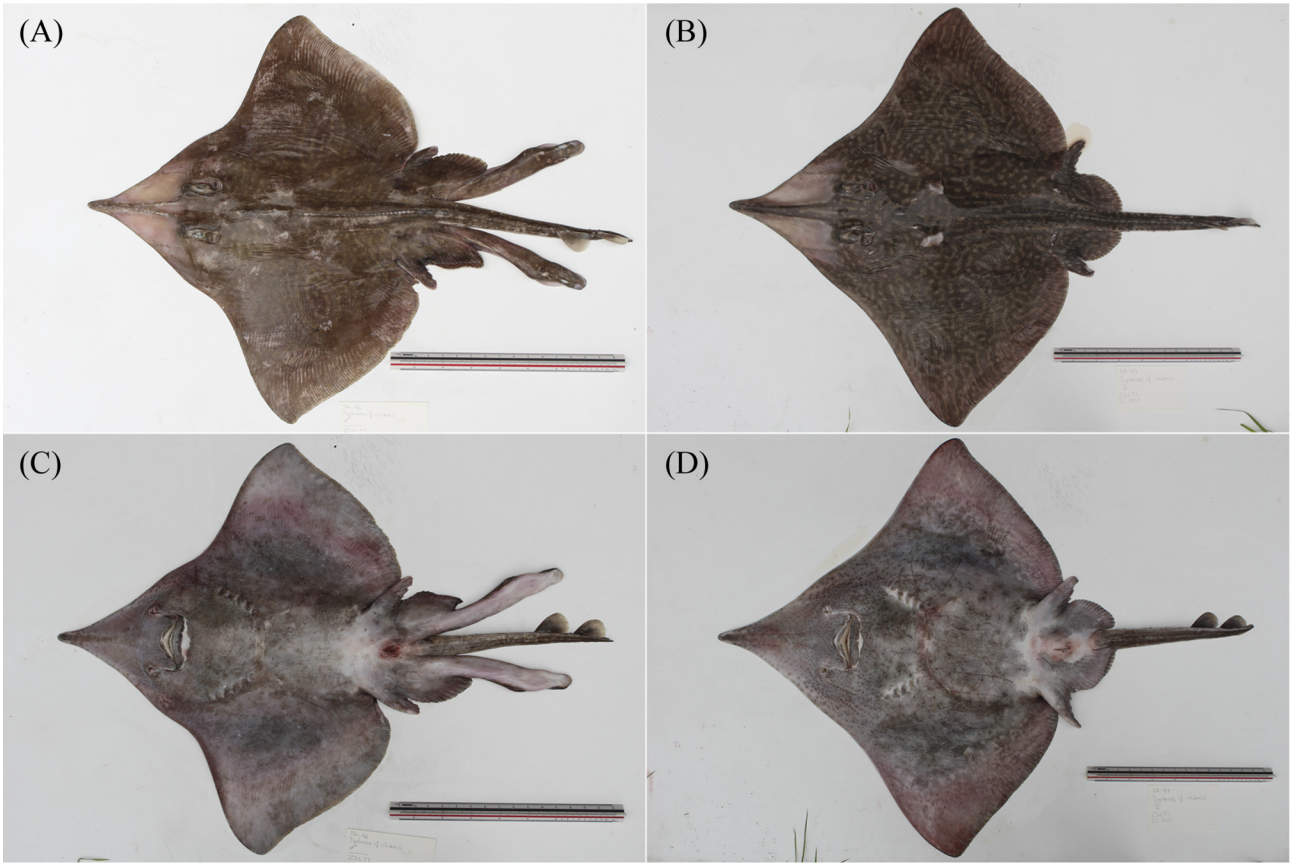

FIGURE 7. Adult specimens of *Dipturus lamillai* **sp. nov.**: (A, C) Dorsal and ventral views of male holotype (MNHNCL ICT 7531; FA-46), respectively. (B, D) Dorsal and ventral views of female paratype (MNHNCL ICT 7532; FA-47), respectively.

Diagnosis. A medium-sized species of *Dipturus*, to at least 107.0 cm TL (FA-7). It is distinguishable from its congeners by the following combination of characters: Dorsal surface of body medium brownish with lighter spots and reticulations ranging from simple (holotype) to complex pattern (female paratype); ocellus in center of each pectoral fin reticulated, margins not well defined. Body, dusky grey ventrally, with light patches around mouth, gills, pelvic girdle, and cloaca; area flanking rostral cartilage membranous and barely translucent; disc relatively broad with angular apices, width 75.2 (73.2; 78.9) % TL; snout elongated. Tail longer in males than in female paratype, 38.4 (37.9) % TL and 35.1% TL, respectively. Ventral head length 36.3 (35.0; 32.7) % TL; pre-orbital

snout length 3.2 (3.1; 3.5) times distance between orbits; orbit diameter 0.4 (0.6; 0.4) times inter-orbital width. Dorsal surface of disc in males with scattered and thick dermal denticles over rostral cartilage; small fine dermal denticles on pre- and post-orbit; thin band of dermal denticles on anterior margins of dorsal fins and anterior margins of disc, and from tip of snout to anterior margin of alar thorn patches; thin band of dermal denticles on anterior margins of dorsal fins. In females, dorsal surface of head and anterior margins of disc with small dermal denticles; narrow patch of dermal denticles on medial-dorsal area between girdles, narrow band on anterior margins of dorsal fins. Both sexes with orbital thorns, single nuchal thorn; scapular thorns lacking; one median row of small caudal thorns; single row of lateral thorns on each side of tail, mostly at anterior part of tail in males and all along tail in female paratype; additional row of small and posteriorly directed thorns above lateral tail fold; malar and alar thorns only in adult males. Ventral sensory pores small, distinct, black-edged, not surrounded by greyish blotches, more abundant anteriorly to gill openings, scarce on abdominal area.

Description. Morphometric and meristic data provided for holotype (mature male FA-46) and two paratypes (mature male FA-39 and mature female FA-47) are expressed as FA-46 (FA-39; FA-47). Information corresponds to fixed and fresh specimens of both sexes unless otherwise indicated. Dorsal surface medium brownish with lighter spots and reticulations, ranging from relatively simple (holotype) to complex in pattern (female paratype); ocellus in center of each pectoral fin reticulated, margins not well defined, with light spots encircled by pattern of lighter broken lines with rosette-like appearance, lighter to undistinguishable when fixed. Reticulated patterns more pronounced in fresh specimens (Fig. 7A–B). Ventral surface dusky grey, with whitish patches around mouth, gills, pelvic girdle and cloaca; ventral surface of claspers whitish (Fig. 7C–D).

Disc rhomboidal, 1.3 (1.4; 1.3) times as broad as long; snout angle in front of spiracles 66.3 (68.7; 71.7) degrees; axis of greatest width 65.3 (65.9; 69.0) % of TL; anterior margin of disc concave anteriorly, moderately convex anterior-laterally to line of orbits, strongly or moderately concave margin just behind line of orbits in males and females, respectively; apex narrowly rounded to sub-angular; posterior margin more convex in males than in females; free rear tip broadly rounded.

Head long, snout narrowly pointed, pre-orbital snout length 7.2 (5.5; 8.7) times orbit length, 3.2 (3.1; 3.5) times distance between orbits; pre-upper jaw length 2.0 (1.8; 2.3) times distance between nostrils. Orbit small, diameter 0.4 (0.6; 0. 4) times distance between orbit width. Spiracles 1.1 (1.7; 1.0) times in orbit diameter; spiracle opening oval (Fig. 8A–B). Nostrils semi-circular (Fig. 8C–D), inner margins forming low semi-circular tube; anterior nasal flap expanded slightly; anterior margin of flap weakly lobe-like. Posterior lobes forming well developed nasal curtain, produced slightly postero-laterally, slightly concave external margins to lobe-like distally, fringed posterior margins, longer in males than in female paratype, reaching lower lip and upper jaw, respectively (Fig. 8C–D). Distance between nostrils 1.6 (1.7–1.7) distance between first gill slits, 1.0 (1.0–1.1) distance between fifth gill slits.

Upper jaw more arched in males than in female paratype; in both sexes, lower jaw convex and indented at symphysis (Fig. 8C–D). Teeth uni-cuspid, with sub-circular bases, arranged in longitudinal rows in both sexes; cusps of medial teeth long, sub-conical, bluntly pointed, posteriorly and lingually directed in both upper and lower jaws; cusps of lateral teeth oblique and almost flat; cusps of males longer and narrower than in females.

Pelvic fins of medium size, deeply forked (Fig. 9A–B); anterior lobe relatively short, slender, bluntly pointed distally 0.7 (0.7–0.8) times posterior lobe, lateral margin entire, inner margin deeply incised; posterior lobe moderately elongate, longer in mature males than in females, 20.7 (20.4–17.8) % of TL, lateral margin weakly convex to straight in males and weakly incised. Claspers elongate, 31.6 (29.4) % TL, moderately robust at shield, slightly depressed at tips; glans noticeably expanded; apopyle and hypopyle visible in external lateral view. Internal components: cleft, shield, slit, spike, spur, and rhipidion; dermal denticles absent (Fig. 9D).

Tail relatively short, length from rear of cloaca to tip 0.6 (0.6; 0.5) times distance from tip of snout to rear of cloaca. Tail narrows posteriorly (Fig. 9A–B), width at pelvic fin axils 1.6 (1.4; 1.4) times width at mid-length, 1.6 (1.7; 1.6) times width at first dorsal fin origin, width 1.7 (1.7; 1.7) times height at insertion of pelvic fin, 2.8 (2.3; 2.8) times height at mid-length, 2.8 (2.6; 2.6) times height at first dorsal fin origin. Tail in males oval at base, more flattened dorsally, more depressed and ventrally flattened at mid-length and triangular with flattened base at inter-dorsal space; in females oval and more equally convex dorsally and ventrally at the base, less expanded at mid-length and triangular at inter-dorsal space. Lateral tail fold narrow, relatively long-based, similar in males and females; originating as a low membranous ridge beside or slightly behind pelvic fin, terminating at tail tip, not obviously broader at any point along its length, maximum width about half height of caudal fin in holotype and about as wide as caudal fin height in female paratype.

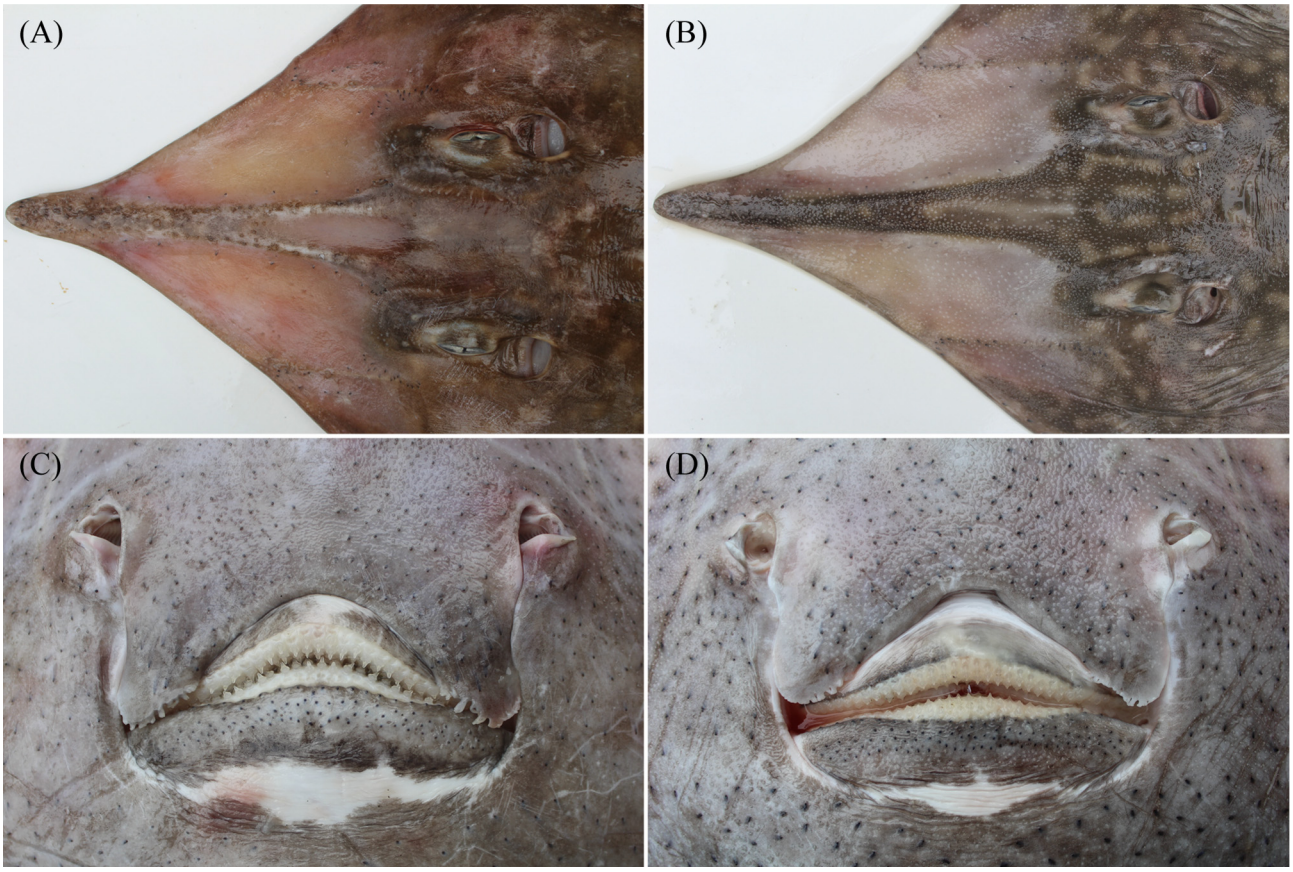

FIGURE 8. Adult specimens of *Dipturus lamillai* **sp. nov.**: (A, C) Dorsal view of head and oro-nasal area of male holotype (MNHNCL ICT 7531; FA-46), respectively. (B, D) Dorsal view of head and oro-nasal area of female paratype (MNHNCL ICT 7532; FA-47), respectively.

Dorsal fins of moderate size, similar shape and size, and not racked (Fig. 10A–B); first dorsal fin slightly taller and more upright than second in holotype; fins subequal in size and similar in shape in paratypes; first dorsal-fin height 1.2 (1.1; 1.1) times in base length; anterior margins of both fins long and weakly convex, apices broadly rounded; posterior margins shorter than anterior margins; free rear tip broadly rounded; second dorsal-fin base slightly shorter in male type specimens and subequal or only marginally longer than first dorsal-fin base in female paratype; inter-dorsal space moderate in type specimens; rear tip of first dorsal fin not overlapping base of second; distance from first dorsal-fin origin to tail tip 2.8 (2.4; 3.0) times first dorsal fin base length, 6.2 (5.2; 5.6) times caudal fin length; first dorsal fin base 2.2 (2.2; 1.9) times caudal-fin length; posterior end of second dorsal fin overlapping with caudal fin origin in both sexes. Epichordal caudal fin lobe present, long-based, low, relatively uniform in height along its length, dorsal margin weakly convex, posterior margin vertical in males, pointed in female paratype, connected sub-basally to second dorsal fin by a low membranous ridge; hypochordal caudal lobe absent. Lateral tail fold subterminal in males and terminal in female paratype (Fig. 10A–B).

Adult males with 5 small orbital thorns with oval base and sharp tips; 2 pre-, 2 mid- and 1 post-orbital; pre- and post-orbital thorns flanked by dermal denticles; female paratype with rosette of 6 orbital thorns; 2 pre-orbital, 3 mid-orbital, and 1 post-orbital (Fig. 8A–B). Malar and alar thorns only in males; malar thorns 6 (10), very sharp, not embedded, not aligned; alar thorns 10 (18), medially-posteriorly directed, set in about 3 longitudinal rows, some embedded, longer than malar thorns, tips very sharp (Fig. 10C–D). Female paratype with single row of 4 median-dorsal thorns and single row of 6 to 8 lateral-dorsal thorns; about 4 posterior-pectoral thorns anterior to rear margin of pectoral fins; few scattered oval-based thorns over pelvic fins (Fig. 11). Caudal thorns of both male type specimens well developed; single row of 20 (25) posteriorly directed caudal thorns extending in linear series of pairs from behind of pelvic girdle area to first dorsal fin; parallel rows of about 6 largely spaced lateral-caudal thorns on each side of central row behind pelvic axil; female paratype with 2 rows of 7 lateral-dorsal thorns behind pectoral girdle; medial-dorsal thorns continuing with caudal thorns; single medial row of 22 caudal thorns, single

row of about 14 lateral-caudal thorns on each side, closely spaced on anterior half of tail, more widely spaced posterior half of tail; additional row of more widely spaced and sharp thorns over lateral tail fold from the line of posterior margin of pelvic fins to second dorsal fin; 3 (2; 2) inter-dorsal thorns.

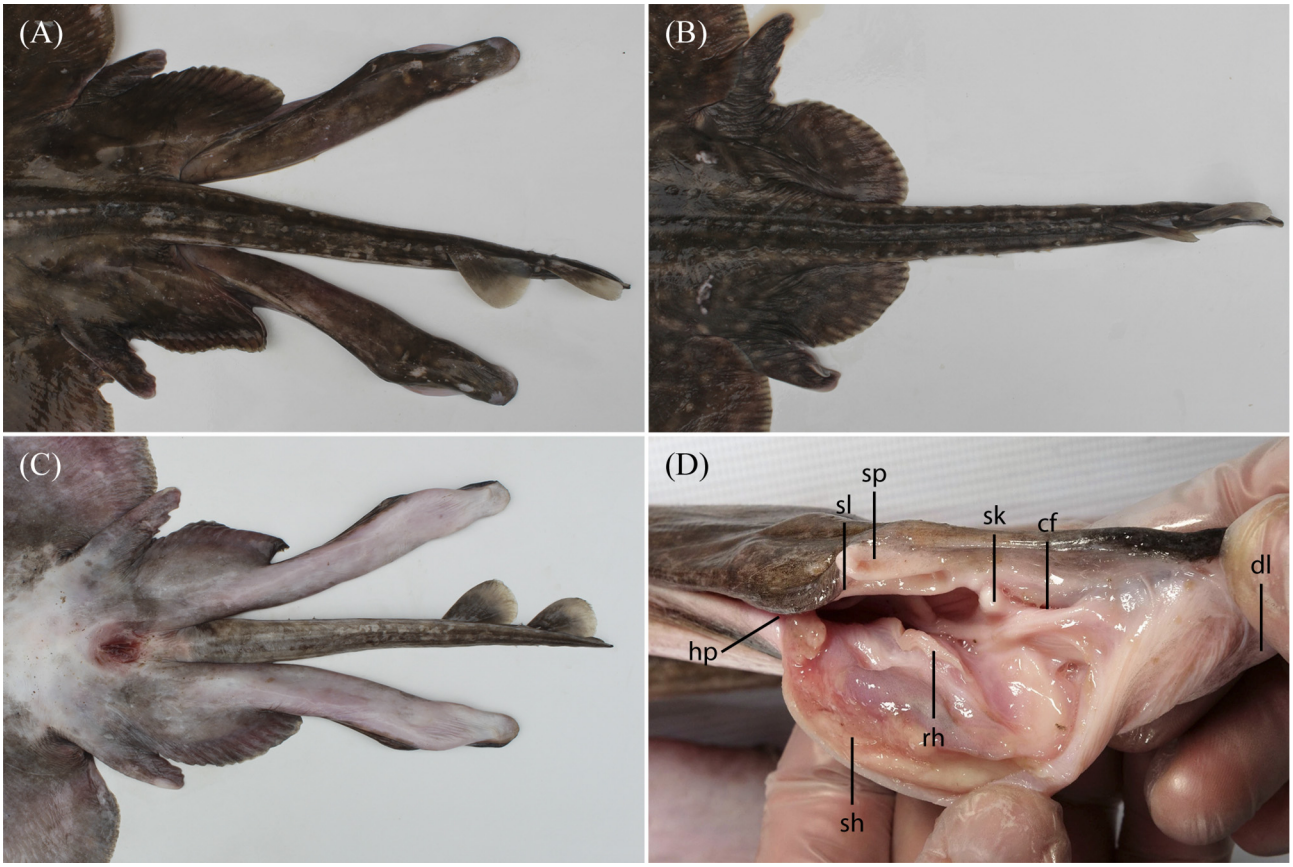

FIGURE 9. Adult specimens of *Dipturus lamillai* **sp. nov.**: (A) Dorsal view of tail of male holotype (MNHNCL ICT 7531; FA-46). (B) Dorsal view of tail of female paratype (MNHNCL ICT 7532; FA-47), (C) Ventral view of claspers of male holotype (MNHNCL ICT 7531; FA-46). (D) Internal components of right clasper of male holotype (MNHNCL ICT 7531; FA-46), lateral view. cf—cleft, dl—distal lobe, hp—hypopyle, rh—rhipidion, sh—shield, sl—slit, sk—spike, and sp—spur.

Dermal denticles of males poorly developed and scarce. In male holotype, small denticles on tip of the snout and over rostral cartilages, 2 small patches in front of orbits, and 1 in front and 1 behind spiracles; dense, narrow band along antero-lateral margin of disc, merging anteriorly to malar thorns, reaching to about half of anterior margin of pectoral fin; maximum width about one-fourth orbit diameter; no denticles on remainder of disc or tail; narrow band of fine denticles on anterior margin of dorsal fins and broadly spaced caudal fin. Ventrally, denticles over most of head, more densely distributed over rostral cartilage and along disc margin to level of about first gill slits. Dermal denticles of female paratype covering most of dorsal surface from snout tip to nuchal thorn, medial-dorsal area and on anterior and upper margins of dorsal and caudal fins; ventrally, dermal denticles cover most of ventral surface of the head including gill openings, sparse over abdomen, slightly dense patch surrounding cloaca; tail lacking dermal denticles.

Meristics. Based on adult male holotype and female paratype in parentheses as follows: tooth rows in upper jaw 38 (35); tooth rows in lower jaw 36 (35). Pectoral-fin propterygial radials 33 (33); mesopterygial radials 15 (14); metapterygial radials 37 (32); total pectoral radials 83 (79). Pelvic-fin radials 20 (20). Trunk vertebrae 25 (27); pre-dorsal caudal vertebrae 61 (62); vertebrae between origins of dorsal fins 29 (18); total vertebrae about 130 (134).

Size. Largest known specimen a female 114.0 cm TL (FA-7, measured fresh), captured at 171 m depth and discarded after measurements were taken.

Distribution. Species known from the slopes of the southwestern Atlantic Ocean adjacent to the Falkland Islands.

Etymology. This species is named in memory of Julio Lamilla, a Chilean biologist who devoted his life to teaching and research focused on the biology and conservation of chondrichthyans, especially batoids. The proposed common name is Warrah skate, or Raya guará, in reference to the extinct Falkland Islands Wolf, the Warrah (*Dusicyon australis* [Kerr 1792]).

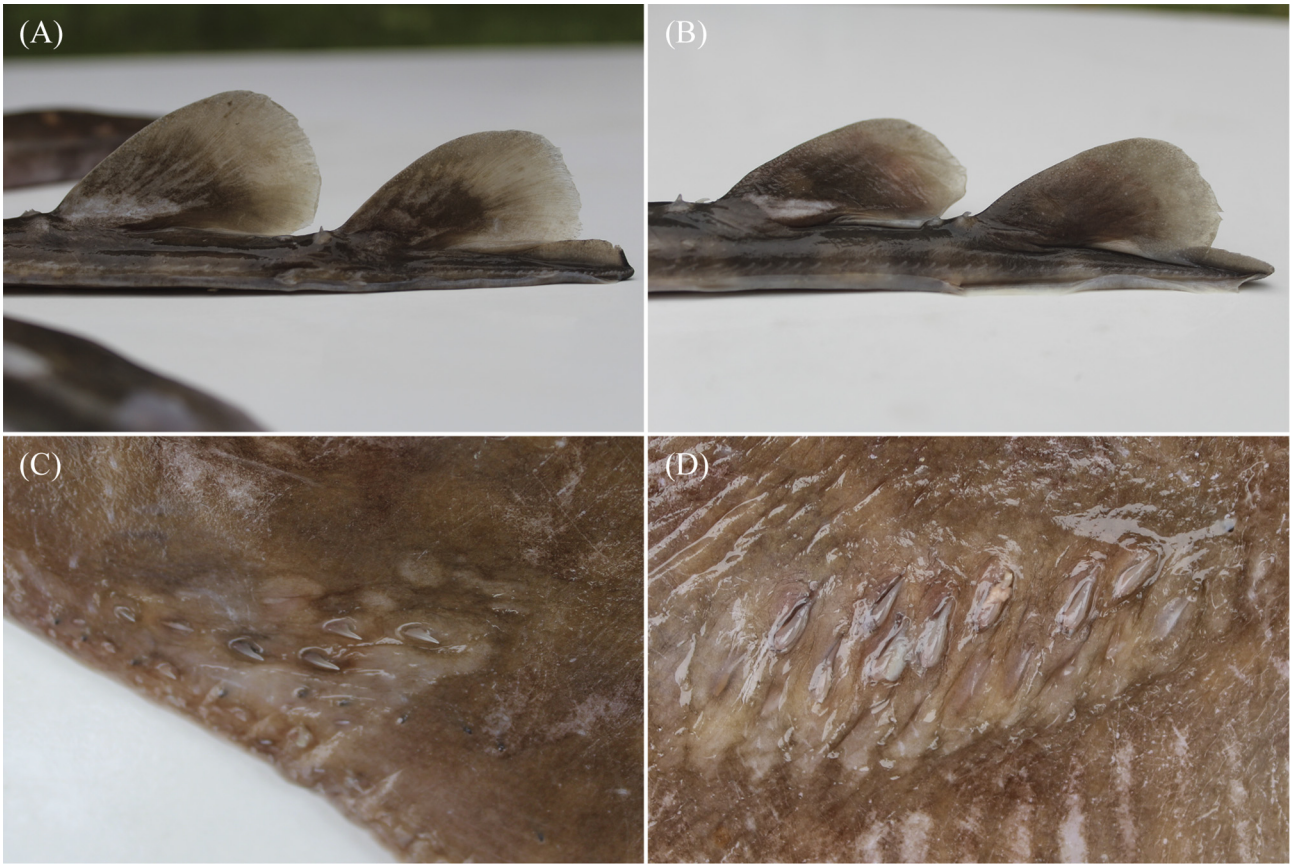

FIGURE 10. Adult specimens of *Dipturus lamillai* **sp. nov.**: (A) Dorsal and caudal fins of male holotype (MNHNCL ICT 7531; FA-46). (B) Dorsal and caudal fins of female paratype (MNHNCL ICT 7532; FA-47). (C, D) Left malar and alar thorns of male holotype (MNHNCL ICT 7531; FA-46), respectively.

Comparisons. Among its congeners, *D. lamillai* **sp. nov.** most closely resembles *D. chilensis*. The two species can be distinguished as follows: whereas the dorsal surface of the disc of *D. lamillai* **sp. nov.** is reticulated in appearance due to the presence of numerous light brown spots that can fuse to form lines, the dorsal surface of the disc of *D. chilensis* is mostly plain brownish with slight mottling. Whereas *D. lamillai* **sp. nov.** bears a dark, reticulated ocellus-like blotch on each pectoral fin, the pectoral fins of *D. chilensis* bear an irregularly shaped purple to red ocellus with solid margins. Furthermore, the distance between the snout tip and cloaca is longer (61.6–64.9 versus 57.8–60.8 % of TL, respectively), while the distance between the cloaca and tail tip is shorter (35.1–38.4 versus 39.2–42.2 % of TL, respectively) in *D. lamillai* **sp. nov.** than in *D. chilensis*. The dermal denticles of both species are similar in size and shape. However, the area covered and the distribution of the denticle patches differ in both sexes between and within species; most conspicuously, the dermal denticles cover a much smaller area of the disc of *D. lamillai* **sp. nov.** in both sexes than they do in *D. chilensis* (Fig. 12C–D).

Dipturus lamillai **sp. nov.** differs from the three other species of *Dipturus* reported from the waters off the Falkland Islands (i.e., *D. argentinensis*, *D. leptocaudus*, and *D. trachydermus*) in the distance between orbits (6.4–(6.4–6.6 versus 5.1, 3.9, and 4.9 % of TL, respectively), in the distance between spiracles (7.7–8.1 versus 6.0, 6.2, and 6.5 % of TL, respectively), and also in mouth width (9.3–10.3 versus 8.1, 7.3, and 8.5 % of TL, respectively). Moreover, both the dorsal and ventral surfaces of the body of *D. lamillai* **sp. nov.** are partially covered with fine dermal denticles whereas those of *D. trachydermus* are almost fully covered with dermal denticles of different sizes.

D. lamillai **sp. nov.** also differs from *D. brevicaudatus* **n. comb.** from the coast of Buenos Aires, Argentina. Based on the original description by Marini (1933), the two species differ in coloration. Whereas the dorsal surface of the disc of *D. lamillai* **sp. nov.** is medium brownish with multiple lighter spots and reticulations, that of *D.*

brevicaudatus **n. comb.** was originally described as uniform brownish, although it was subsequently redescribed (under the name *Zearaja brevicaudata*) as grayish by Gabbanelli *et al*. (2018). However, morphometric comparisons are difficult to make between *D. lamillai* **sp. nov.** and the recently resurrected *D. brevicaudatus* **n. comb.** as redescribed by Gabbanelli *et al.* (2018). This is largely because the measurements presented by these authors are combined for juvenile, subadult, and adult specimens of both sexes, and thus do not allow for comparisons of specimens of the same size or same sex of both species. In addition, although measurements are presented for the holotype specimen, that specimen is a juvenile female (32.4 cm in TL) and those measurements are not comparable to those for the holotype of *D. lamillai* **sp. nov.**, which is an adult male.

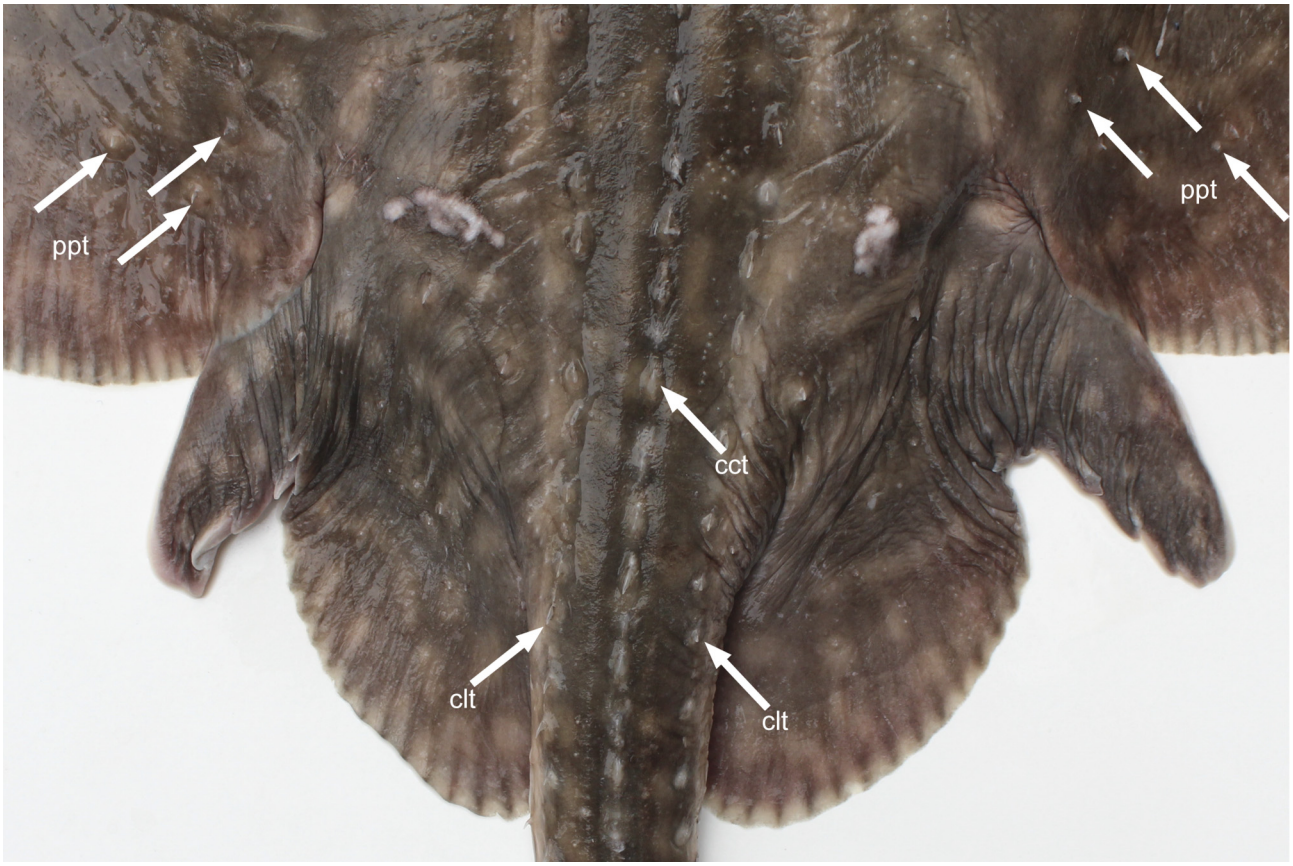

FIGURE 11. Adult specimen of female paratype (MNHNCL ICT 7532; FA-47) of *Dipturus lamillai* **sp. nov.**: Dorsal view of posterior angle of pectoral fins, and anterior and posterior lobes of pelvic fins. Thorns indicated with arrows. clt—caudal-lateral thorns, cct—caudal-central thorns, and ppt—posterior pectoral thorns.

Molecular analysis. Intraspecific p-distances across the 1,043 bp of NADH2 sequence were as follows: *D. chilensis* (n=12) 0–5 bp, with a mean of 2.7 bp; *D. lamillai* **sp. nov.** (n=9) 0–4 bp, with a mean of 1.6 bp; *D. nasutus* (n=3) 0–2 bp with a mean of 1.3 bp. Interspecific p-distances were as follows: *D. lamillai* **sp. nov.** and *D. chilensis* 28–32 bp with a mean of 29.4 bp; *D. lamillai* **sp. nov.** and *D. nasutus* 33–35 bp with a mean of 33.4; *D. chilensis* and *D. nasutus* 8–14 bp with a mean of 11.1 bp.

The Neighbor-Joining tree resulting from analysis of NADH2 data is shown in Figure 13. Our eight specimens of *D. lamillai* **sp. nov.** from the Falkland Islands were found to cluster together away from the cluster composed of our three specimens of *D. nasutus* from New Zealand and the cluster composed of our 11 specimens of *D. chilensis* from Chile. GenBank specimen No. KJ913073, collected from Chile by Vargas-Caro *et al*. (2016a), was found to nest among the latter specimens. However, GenBank specimen No. KF748508, collected from raw fillets at a skate restaurant in Seoul, Korea (Jeong & Lee 2016), was found to nest among our specimens of *D. lamillai* **sp. nov.**

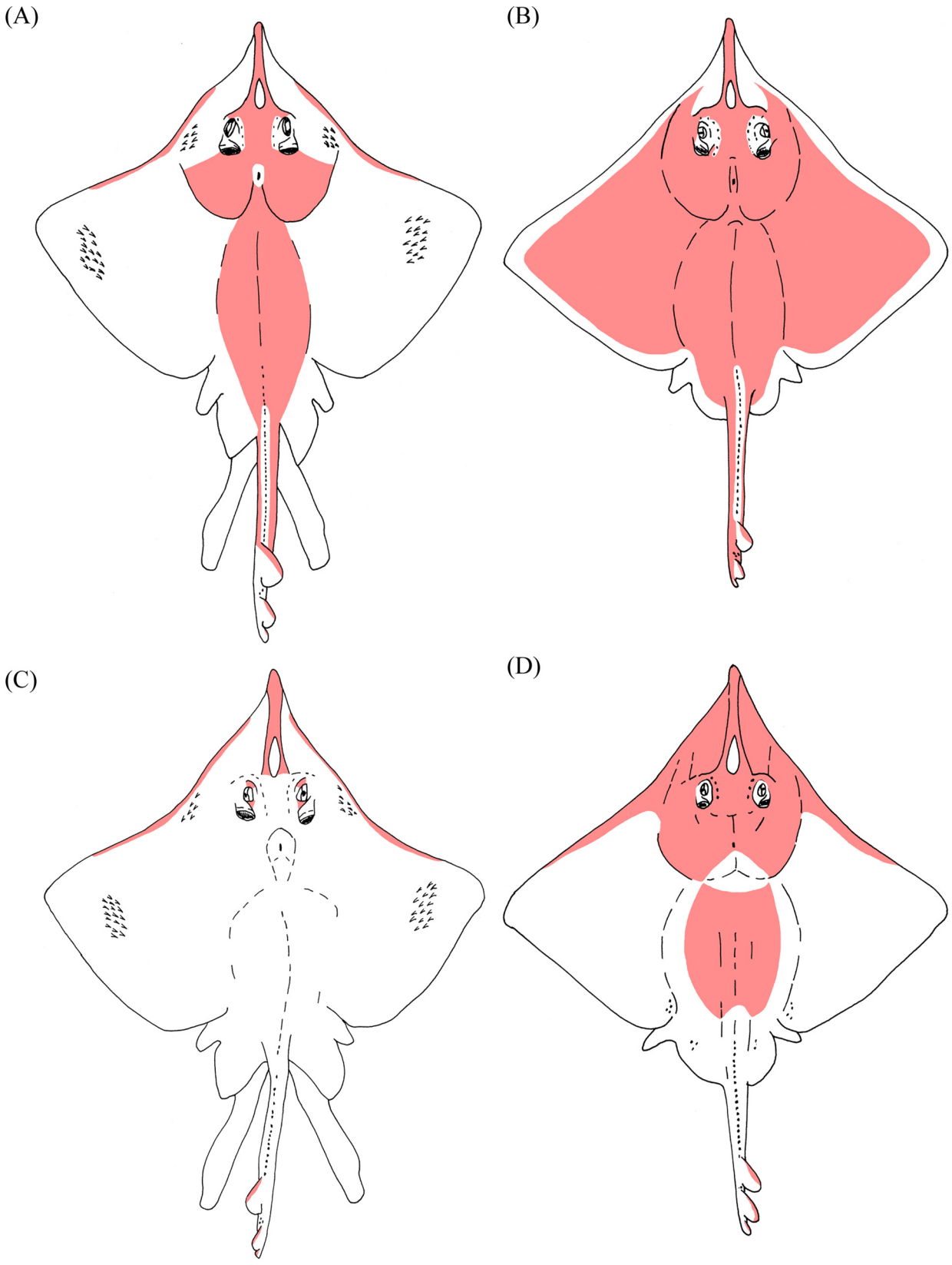

FIGURE 12. Line drawings depicting areas covered by dermal denticles in dorsal view of adults of (A, B) male and female of *Dipturus chilensis*, respectively, and (C, D) male and female of *Dipturus lamillai* **sp. nov.**, respectively.

TABLE 2. Morphometrics for neotype (CHL-88), and male and female voucher specimens (CHL-138 and CHL-89, respectively) of *Dipturus chilensis*, and for holotype (FA-46) and male and female paratypes (FA-39 and FA-47, respectively) of *D. lamillai* **sp. nov.** Measurements are expressed as a percentage of total length.

	CHL-88		CHL-138		CHL-89		FA-46		FA-39		FA-47	
	♂	%TL	♂	%TL	♀	%TL	♂	%TL	♂	%TL	♀	%TL
Total length (mm)	90.7		94.9		73.5		78.7		91.5		94.0	
Disc width		76.4		75.0		77.0		75.2		73.2		78.9
Disc length (direct)		60.5		61.4		62.9		63.8		59.3		65.5
Snout to maximum disc width		38.8		37.3		40.1		41.7		39.1		45.2
Snout length (pre-orbital direct)		16.4		18.0		19.7		20.2		19.7		23.4
Snout to spiracle		21.1		23.0		26.5		23.5		23.7		26.3
Head length (dorsal)		23.2		25.6		27.1		27.2		25.4		28.2
Orbit diameter		3.3		2.9		3.9		2.8		3.6		2.7
Orbit and spiracle length		5.7		5.3		6.7		5.0		5.8		5.4
Spiracle length		2.6		2.3		2.9		2.7		2.1		2.7
Distance between orbits		6.8		6.1		6.9		6.4		6.4		6.6
Distance between spiracles		7.7		7.3		7.7		7.8		8.1		7.7
Snout base width at spiracles		30.7		29.8		36.1		29.7		30.6		37.2
Snout to spiracle (straight)		18.5		20.7		23.4		22.7		22.4		25.7
Snout to cloaca (first hemal spine)		57.8		59.5		60.8		61.6		61.7		64.9
Cloaca to caudal-fin tip		42.2		40.5		39.2		38.4		38.3		35.1
Ventral snout length (pre-upper jaw)		13.0		15.7		18.6		19.1		17.5		22.0
Pre-nasal length		12.9		15.4		18.0		17.9		16.7		20.7
Ventral head length (to fifth gill)		35.1		34.2		37.7		36.3		35.0		32.7
Mouth width		10.6		9.5		10.2		9.3		9.7		10.3
Distance between nostrils		9.6		9.4		10.1		9.4		9.6		9.7
Nasal curtain length		3.6		5.4		4.4		4.9		4.7		5.0
Nasal curtain (total width)		11.8		9.2		11.7		10.2		11.4		10.0
Nasal curtain (min. width)		8.1		4.5		7.8		7.1		9.2		7.0
Nasal curtain (lobe width)		1.9		2.1		2.2		2.3		2.2		2.1
Width of first gill opening		2.0		1.9		1.9		2.0		1.5		2.1
Width of fifth gill opening		1.6		1.6		1.9		1.7		1.7		2.0
Distance between first gill openings		20.4		1.9		21.0		15.0		16.4		16.0
Distance between fifth gill openings		11.0		1.7		12.4		9.4		9.8		11.1
Length of anterior pelvic lobe		11.9		11.0		13.5		14.2		13.4		13.3
Length of posterior pelvic lobe		20.3		18.5		16.9		20.7		20.4		17.8
Pelvic base width		8.4		15.6		10.2		9.4		9.6		10.9
Clasper (post-cloacal length)		30.7		31.0		0.0		31.6		29.4		NA
Cloaca to pelvic-clasper insertion		10.9		2.9		0.0		11.9		11.4		NA
Tail at axil of pelvic fins (width)		2.9		3.5		3.6		4.1		4.0		3.9
Tail at axil of pelvic fins (height)		2.5		2.5		2.4		2.4		2.4		2.3
Tail at mid-length (width)		2.7		2.7		2.6		2.6		3.0		2.7
Tail at mid-length (height)		1.4		1.7		1.4		1.4		1.7		1.4
Tail at D1 origin (width)		2.2		2.1		2.4		2.5		2.4		2.4
Tail at D1 origin (height)		1.5		1.6		1.5		1.5		1.5		1.5

.....continued on the next page

TABLE 2. (Continued)

	CHL 88		CHL-138		CHL 89		FA-46		FA-39		FA-47	
	♂	%TL	♂	%TL	♀	%TL	♂	%TL	♂	%TL	♀	%TL
D1 base length		6.5		5.4		5.4		5.1		5.3		4.3
D1 height		3.7		4.2		3.0		4.3		3.2		3.9
D1 origin to caudal-fin tip		17.6		15.7		14.7		14.3		12.6		12.9
D2 base length		4.2		3.1		5.3		5.0		4.5		4.5
D2 origin to caudal-fin tip		12.1		8.9		8.7		6.6		6.9		7.1
Caudal-fin length		4.9		4.1		3.9		2.3		2.4		2.3
Caudal-fin height		0.5		0.9		0.5		0.7		0.6		0.2
Lateral tail fold length		3.6		34.6		32.7		34.1		31.0		29.6
Lateral tail fold middle width		0.3		0.2		0.2		0.4		0.2		0.4
Tail width at caudal fin origin		1.3		0.5		1.3		0.4		0.8		0.8

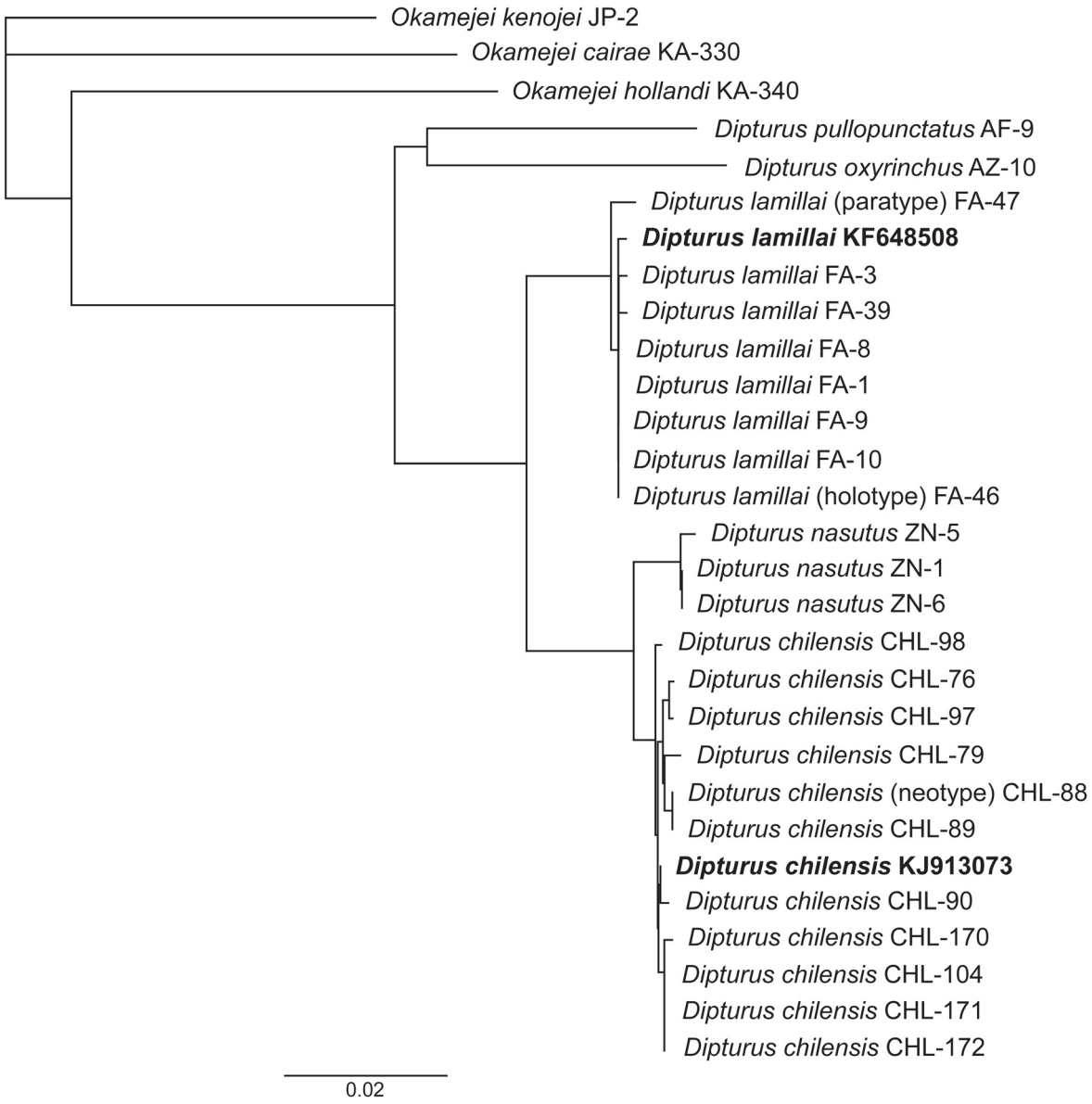

FIGURE 13. Neighbor-Joining tree generated with Jukes-Cantor genetic distance model of sequence data for 1,043 base pairs of the NADH2 gene. Sequences obtained from GenBank are shown in bold.

Discussion

Analysis of NADH2 data confirm our morphological results, which indicate that *D. lamillai* **sp. nov.** represents a species distinct from *D. chilensis*. Not only did specimens of these species cluster in separate groups in the tree resulting from the Neighbor-Joining analysis, but their NADH2 sequences differed by an average of 29.4 bp across specimens of the two species; this is in contrast to the 0–5 bp differences among specimens of each species. Our results also confirm that the specimen from which the mitochondrial genome sequence data registered in GenBank under No. KJ913073 (as *Zearaja chilensis*) were generated, represents the species now referred to as *D. chilensis*. In contrast, our results indicate that the specimen from which the mitochondrial genome sequence data registered in GenBank under No. KF648508 (also identified as *Zearaja chilensis*) were generated was actually a specimen of *D. lamillai* **sp. nov.** This finding serves to emphasize the importance of confirming the identity and provenance of specimens for which sequence data are generated and submitted to GenBank.

Our results also provide molecular and morphological support for the recognition of *Zearaja* as a junior synonym of *Dipturus*. As was the case in the analyses of Naylor *et al*. (2012b), we found specimens of species assigned to *Zearaja* by Last & Gledhill (2007), which included the type species *Z. nasuta*, to nest among species of *Dipturus* in the tree resulting from our molecular analysis. Furthermore, beyond a relatively simple clasper morphology, which unites a subclade of *Dipturus* species, the morphological features considered by Last & Gledhill (2007) to distinguish the two genera are actually known to occur in at least some other members of Dipturus.

Surprisingly little variation in NADH2 sequence was found across the specimens of *D. chilensis* included in our analysis despite the fact that these specimens were collected from as far north as Valparaíso and as far south as Punta Arenas (see Fig. 1). In fact, the amount of variation seen among the six specimens from Valparaíso (i.e., 0–4 bp) was the same as that seen between these specimens and those from Punta Arenas.

Our work has obvious implications for management and conservation concerns surrounding what are now recognized as two commercially important skate species. First, the distribution of *D. chilensis* is much more restricted than previously thought; it appears to occur only on the west coast of South America. Second, the distribution of *D. lamillai* **sp. nov.** may be even more limited, depending on more detailed study of skates traditionally assigned to *D. chilensis* collected from the continental shelf of the eastern coast of South America. As it stands, *D. lamillai* **sp. nov.** is known only from the waters surrounding the Falkland Islands.

Acknowledgements

We thank the Fisheries Department of the Falkland Islands, especially Alexander Arkhipkin, for allowing the first author to join the Research Cruise ZDLT1-11-2013 Skate Biomass and Biological Survey on the FV Castelo in 2013 and for providing logistical support, and the officers and crew for all of their assistance on board. We are also grateful for all the support provided by the staff of Instituto de Fomento Pesquero in Chile, and especially to Eric Daza and Edison Garcés for their valuable help in collecting skates from Punta Arenas. We want to acknowledge Augusto Cornejo (National Museum of Natural History of Santiago, Chile) for his constant help in taking care of the newly collected material from Chile and the Falkland Islands. We are grateful to Hannah Ralicki for generating a portion of the NADH2 sequence data and to Elizabeth Jockusch for the use of her laboratory for the molecular work, as well as for designing the ILEM_SeqF and ASNM_SeqR primers. We also thank Dave Catania and Jon Fong from the California Academy of Sciences for their valuable help in generating x-rays images of specimens from Chile and the Falkland Islands. Beth Barbeau (UConn), Don Gabriel Rojas, and Marcelo Yáñez provided valuable help and suggestions on the figures. We are grateful to Kirsten Jensen for comments on the manuscript. Finally, the first author would like to thank LTC Katherine Barozzi and SGM Erwin Azócar (Chilean Army) for their logistical support in Punta Arenas. The first author received support from Fulbright Chile, Faculty Development Program award, as well as from the Comisión Nacional de Investigación Científica y Tecnológica, CONICYT Becas Chile award. This work was supported in part with funds from National Science Foundation Awards Nos. 1457762 and 1457776. Any opinions, findings, conclusions, or recommendations expressed in this material are those of the authors and do not necessarily reflect the views of the National Science Foundation.

References

Bigelow, H. & Schroeder, W. (1951) Three new skates and a new chimaerid fish from the Gulf of Mexico. *Journal of the Washington Academy of* Sciences, 41 (12), 383–392.

Bigelow, H. & Schroeder, W. (1962) New and little known batoid fishes from the Western Atlantic. *Bulletin of the Museum of Comparative Zoology*, 128 (4), 161–244.

Concha, F., Ebert, D. & Long, D. (2016) *Notoraja martinezi* sp. nov., a new species of deepwater skate and the first record of the genus *Notoraja* Ishiyama, 1958 (Rajiformes: Arhynchobatidae) from the eastern Pacific Ocean. *Zootaxa*, 4098 (1), 179–190.

Concha, F., Morales, N. & Hernández, S. (2018) First observations on captive hatching and incubation period of the yellownose skate Dipturus chilensis (Rajiformes: Rajidae), from the South-Eastern Pacific Ocean. *Journal of Fish Biology*, 93 (4), 738–740.
https://doi.org/10.1111/jfb.13765

Concha, F., Oddone, M., Bustamante, C. & Morales, N. (2012) Egg capsules of the yellownose skate *Zearaja chilensis* (Guichenot 1848) and the roughskin skate *Dipturus trachyderma* (Krefft and Stehmann 1974) (Rajiformes: Rajidae) from the south-eastern Pacific Ocean. *Ichthyological Research*, 59 (4), 323–327.
https://doi.org/10.1007/s10228-012-0293-z

Cousseau, M., Figueroa, D., Díaz de Astarloa, J., Mabragaña, E. & Lucifora, L. (2007) Rayas, chuchos y otros batoideos del Atlántico Sudoccidental (34 S–55 S). *Instituto Nacional de Investigación y Desarrollo Pesquero INIDEP*, Mar del Plata, 100 pp.

Díaz de Astarloa, J., Mabragaña, E., Hanner, R. & Figueroa, D. (2008) Morphological and molecular evidence for a new species of longnose skate (Rajiformes: Rajidae: *Dipturus*) from Argentinean waters based on DNA barcoding. *Zootaxa*, 1291, 35–46.

Ebert, D. & Compagno, L. (2007) Biodiversity and systematics of skates (Chondrichthyes: Rajiformes: Rajoidei). *Environmental Biology of Fishes*, 80, 111–124.
https://doi.org/10.1007/s10641-007-9247-0

Ebert, D., Compagno, L. & Cowley, P. (2008) Aspects of the reproductive biology of skates (Chondrichthyes: Rajiformes: Rajoidei) from southern Africa. *ICES Journal of Marine Science*, 65, 81–102.
https://doi.org/10.1093/icesjms/fsm169

Fuentealba, M. & Leible, M. (1990) Perspectivas de la pesquería de la raya volantín *Raja* (*Dipturus*) *flavirostris*: Estudio de edad, crecimiento y algunos aspectos reproductivos. *In:* Barbieri, M.A. (Ed.) *Perspectivas de la Actividad Pesquera en Chile*. Escuela de Ciencias del Mar, Universidad Católica de Valparaíso, pp. 227–236.

Gabbanelli, V., Díaz de Astarloa, J., González-Castro, M., Vázquez, D. & Mabragaña, E. (2018) Almost a century of oblivion: Integrative taxonomy allows the resurrection of the longnose skate *Zearaja brevicaudata* (Marini, 1933) (Rajiformes; Rajidae). *Comptes Rendus Biologies*, 341 (9–10), 454–470.
https://doi.org/10.1016/j.crvi.2018.10.002

Gomes, U. & Paragó, C. (2001) Especie nova de rajideo (Chondrichthyes, Rajiformes) do Atlantico Sul Ocidental. *Boletim do Museo Nacional,* 448, 1–10.

Gomes, U. & Picado, S. (2001) Distribution of the species of *Dipturus* Rafinesque (Rajidae, Rajinae, Rajini) off Brazil and first record of the Caribbean skate *D. teevani* (Bigelow & Schroeder), in the Western South Atlantic. *Revista Brasileira de Zoologia*, 18 (1), 171–185.
https://doi.org/10.1590/S0101-81752001000100021

Hulley, P. (1970) An investigation of the Rajidae of the west and south coasts of southern Africa. *Annals of the South African Museum*, 55 (4), 151–220.

Hulley, P. (1972) The origin, interrelationship and distribution of Southern African Rajidae (Chondrichthyes, Batoidei). *Annals of the South African Museum*, 60 (1), 1–103.

Ishihara H. (1987) Revision of the Western North Pacific species of the genus *Raja*. *Japanese Journal of Ichthyology*, 34 (3), 241–285.
https://doi.org/10.1007/BF03380117

Jeong, D. & Lee, Y. (2016) Complete mitochondrial genome of the Yellownose skate: *Zearaja chilensis* (Rajiformes, Rajidae), *Mitochondrial DNA Part A*, 27 (1), 293–294.

Jukes, T. & Cantor, C. (1969) Evolution of protein molecules. *In* Munro, H. N. (Ed.), *Mammalian Protein Metabolism*, Academic Press, New York, pp. 21–132.
https://doi.org/10.1016/B978-1-4832-3211-9.50009-7

Krefft, G. & Stehmann, M. (1975) Ergebnisse der Forschungsreisen des FFS "Walter Herwig" nach Südamerika. XXXVI. Zwei weitere neue Rochenarten aus dem Südwestatlantik *Raja (Dipturus) leptocaudus* und *Raja (Dipturus) trachyderma* spec. nov. (Chondrichthyes, Batoidei, Rajidae). *Archiv für Fischereiwissenschaft*, 26 (3), 77–97.

Last, P.R. & Gledhill, D.C. (2007) The Maugean skate, *Zearaja maugeana* sp. nov. (Rajiformes: Rajidae)—a micro-endemic, Gondwanan relict from Tasmanian estuaries. *Zootaxa*, 1494, 45–65.

Last, P.R. & Yearsley, G. (2002) Zoogeography and relationships of Australasian skates (Chondrichthyes: Rajidae). *Journal of Biogeography*, 29, 1627–1641.

https://doi.org/10.1046/j.1365-2699.2002.00793.x
Last, P.R., White, W.T., Carvalho, M.R. de, Séret, B., Stehmann, M.F.W. & Naylor, G.J.P. (Eds.) (2016) Rays of the World. CSIRO Publishing, Melbourne, 790 pp.
Last, P.R., White, W.T., Pogonoski, J.J. & Gledhill, D.C. (2008) New Australian skates (Batoidea: Rajoidei)—background and methodology. *In*: Last, P.R., White, W.T., Pogonoski, J.J. & Gledhill, D.C. (Eds.), *Descriptions of New Australian Skates (Batoidea: Rajoidei)*. CSIRO Marine & Atmospheric Research Paper 021, pp. 1–8.
Leible, M. (1987) Taxonomic description of juveniles and adults of *Raja* (*Dipturus*) *flavirostris* Philippi, 1892 (Rajiformes: Rajidae) captured in front of the coast off central Chile. *Gayana Zoología*, 51, 131–176.
Licandeo, R. & Cerna, F. (2007) Geographic variation in life-history traits of the endemic kite skate *Dipturus chilensis* (Batoidea: Rajidae), along its distribution in the fjords and channels of southern Chile. *Journal of Fish Biology*, 71, 421–440.
https://doi.org/10.1111/j.1095-8649.2007.01499.x
Licandeo, R., Cerna, F. & Céspedes, R. (2007) Age, growth, and reproduction of the roughskin skate, *Dipturus trachyderma*, from the southeastern Pacific. *ICES Journal of Marine Science*, 64,141–148.
https://doi.org/10.1093/icesjms/fsl012
Licandeo, R., Lamilla, J., Rubilar, P. & Vega, R. (2006) Age, growth, and sexual maturity of the yellownose skate *Dipturus chilensis* in the south-eastern Pacific. *Journal of Fish Biology*, 68, 488–506.
https://doi.org/10.1111/j.0022-1112.2006.00936.x
Marini, T. (1933) Rectificando errores ictiológicos. *Physis*, 11 (1933), 328–332.
McEachran, J. & Dunn, K. (1998) Phylogenetic analysis of skates, a morphologically conservative clade of elasmobranchs (Chondrichthyes: Rajidae). *Copeia*, 1998 (2), 271–290.
https://doi.org/10.2307/1447424
Menni, R., Jaureguizar, A., Stehmann, M. & Lucifora, L. (2010) Marine biodiversity at the community level: Zoogeography of sharks, skates, rays and chimaeras in the southwestern Atlantic. *Biodiversity Consevation*, 19 (3), 775–796.
https://doi.org/10.1007/s10531-009-9734-z
Naylor, G.J.P., Caira, J.N., Jensen, K., Rosana, K.A.M., White, W.T. & Last, P.R. (2012a) A DNA sequence–based approach to the identification of sharks and ray species and its implications for global elasmobranch diversity and parasitology. *Bulletin of the Museum of Natural History*, 367, 262 pp.
Naylor, G.J.P., Caira, J.N., Jensen, K., Rosana, K.A.M., Straube, N. & Lakner, C. (2012b) Elasmobranch phylogeny: A mitochondrial estimate based on 595 species. *In* Carrier, J., Musick, J., and Heithaus, E. (Eds.), *The Biology of Sharks and Their Relatives*, CRC Press, Boca Raton, pp. 31–56.
Naylor, G.J.P., Ryburn, J.A., Fedrigo, O.J. & López, J.A. (2005) Phylogenetic relationships among the major lineages of modern elasmobranchs. *In*: Hamlett W. (Ed.), *Reproductive Biology and Phylogeny of Chondrichthyes: Sharks, Batoids, and Chimaeras, Vol. 3.* Science Publishers, Enfield, pp. 1–26.
Pompert, J., Brewin, P., Winter, A. & Blake, A. (2014) Scientific Report, Fisheries Cruise ZDLT1-11-2013. Stanley, Fisheries Department, Directorate of Natural Resources, Falkland Islands Government, 100 pp.
Rafinesque, C. (1810) Caratteri di alcuni nuovi generi e nuove specie di animali e piante della Sicilia, con varie osservazioni sopra i medisimi. Sanfilippo, Palermo. (Part 1 involves fishes, pp. [i–iv] 3–69, Part 2 with slightly different title, pp. ia–iva + 71–105). Pls. 1–20.
Vargas-Caro, C., Bustamante, C., Bennett, M. & Ovenden, J. (2016a) The complete validated mitochondrial genome of the yellownose skate *Zearaja chilensis* (Guichenot 1848) (Rajiformes, Rajidae). *Mitochondrial DNA Part A*, 27 (2), 1227–1228.
Vargas-Caro, C., Bustamante, C., Lamilla, J. & Bennett, M. (2015) A review of longnose skates *Zearaja chilensis* and *Dipturus trachyderma* (Rajiformes: Rajidae). *Universitas Scientiarum*, 20 (3), 321–359.
https://doi.org/10.11144/Javeriana.SC20-3.arol
Vargas-Caro, C., Bustamante, C., Lamilla, J., Bennett, M. & Ovenden, J. (2016b) The phylogenetic position of the roughskin skate *Dipturus trachyderma* (Krefft & Stehmann, 1975) (Rajiformes, Rajidae) inferred from the mitochondrial genome. *Mitochondrial DNA*, *Part A*, 27 (4), 2965–2966.
Whitley, G. (1939) Taxonomic notes on sharks and rays. *Australian Zoologist*, 9 (3), 227–262.